FABRICATION AND PRODUCTION PROTOCOL FOR CAPILLARY ULTRAFILTRATION MEMBRANES AND MODULES

EP Jacobs · C Yanic · SM Bradshaw ·
C Marais · MW Bredenkamp · P Swart

WRC Report No. 769/1/03

Water Research Commission

FABRICATION AND PRODUCTION PROTOCOL FOR CAPILLARY ULTRAFILTRATION MEMBRANES AND MODULES

Final Report to the

Water Research Commission

by

Jacobs EP[1], Yanic C[1], Bradshaw SM[2], Marais C[2]
Bredenkamp MW[3], and Swart P[4]

[1]Institute for Polymer Science, [2]Department of Chemical Engineering
[3]Department Organic Chemistry, [4]Department Biochemistry
University of Stellenbosch
Private Bag X1, Matieland, 7600

WRC Report No 769/1/03
ISBN 1-86845-843-1

February 2003

Disclaimer

This report emanates from a project financed by the Water Research Commission (WRC) and is approved for publication. Approval does not signify that the contents necessarily reflect the views and policies of the WRC or the members of the project steering committee, nor does mention of trade names or commercial products constitute endorsement or recommendation for use.

Printed by Silowa Printers

Acknowledgements

The project team wishes to thank the following persons for their valuable input and support:

The WRC Steering Committee that consisted of the following persons:
Dr G Offringa (Chair)
Mr OCE Hempel (Secretary)
Dr JJ Schoeman
Mr DJC Nel (alternate: Mr H Strohwald)
Dr VL Pillay
Prof P Swart
Prof RD Sanderson
Prof PD Rose
Prof SM Bradshaw

Membrane evaluation was conduced by a number of researchers and in a variety of applications and capacities. The project team would like to express appreciation the following persons for their efforts and valuable feedback: Dr VL Pillay (Durban Institute of Technology, former ML Sultan Technikon), Dr B Odhav (Durban Institute of Technology, former ML Sultan Technikon), Mr B Hendry (Peninsula Technikon), Prof F Petersen (Cape Technikon), Dr W Leukes (Rhodes University) and Dr S Burton (Rhodes University).

The service of the Central Mechanical Services Dept of the Faculty of Engineering, University of Stellenbosch, is appreciated and the valuable support of Mr H Foot, J Weerdenberg and G Treurnicht, amongst others, is acknowledged.

We are grateful to Doug Peet and Associates for valuable support with respect to mould and other design work and fabrication.

Not least and kept for last: It is very necessary to thank Deon Koen for his various contributions in the field of membrane and module development over the past number of years.

Executive summary

Background and objectives

Capillary membranes are narrow-bore tube like membranes. These membranes are self-supporting, that is, their construction is such that they can withstand pressurisation from within or from the outside without collapsing or bursting. Typical operating pressures are below 2bar. Because the membranes are self-supporting, it is possible to reverse the flow across the wall of the membranes by reversing the pressure differential. This effectively allows the membranes to be back-flushed, a process whereby foulants that have accumulated on the membrane surface may be dislodged and rinsed from within the membrane tube. The membranes are housed in shell-and-tube modules, which is relatively easy to construct.

At the start of the project the knowledge to produce skinless ultrafiltration membranes from polysulphone was in place (WRC project 632). Techniques were also devised in the same project to construct 90mm modules ($5m^2$ membrane area) within which to house the membranes for use. However, further improvement of both the membrane and module was deemed necessary before the technology could be regarded as acceptable for application and commercialisation.

The objectives set for this project were in essence therefore formulated in order to further capillary membrane technology towards application and commercial acceptance.

The original aims of the project, as set out in the research contract, can be subdivided into three categories. These, as well as the individual aims, are listed below.

Capillary membrane production development

- Devise a fabrication protocol to produce capillary membranes with enhanced separation properties for use in water filtration and extractive adsorption of contaminants in aqueous streams.

- Develop a fabrication protocol to produce capillary membranes with special functionality to enable enzymes to be immobilised in a membrane bioreactor for the treatment of aqueous effluent or other product/process stream.

Membrane modification

- Expand the range of neutral surface adsorptive coating materials to include materials with cationic or anionic moieties.

- Devise a simple protocol to modify the surface chemistry of operational membranes by adsorptive techniques to improve their anti-fouling characteristics and operating flux.

- Integrate membrane surface modification with cleaning protocol and determine the efficacy of such a combined approach in difficult applications.

Axial-flow module and manifold development

- Improve and upscale the design of prototype and semi-production 50m^2 axial-flow capillary membrane modules for use in low-cost treatment operations.

- Improve and upscale the design of prototype and semi-production transverse flow modules to capitalise on the greater back-mixing properties of this type of membrane device.

Research initiatives were initiated during the course of the project to test the integrity of both membranes and modules that were developed during this project. For that reason the project was closely aligned with WRC projects K5/965 (*Capillary ultrafiltration membrane process and systems R&D)*, K5/1070 *(The development of small-system ultrafiltration systems for potable water production)* and K5/1034 (*Microbiological performance criteria for membrane technology for wastewater treatment*) towards the end.

Capillary membrane production development

Past research focussed on the development of an outer skinless polysulphone membrane. This specially developed membrane is now used in studies on the continuous production of enzymes by filamentous fungi in a membrane bioreactor application. The low-pressure membrane that resulted had very high specific-flux values, typically 2 to 4 Lmh/kPa[v], and PEG35000[§] molecular mass cut-off values of less than 80%.

The skinless membrane was also extensively used in laboratory and field evaluations for potable water production. The membranes performed well, especially concerning water flux and colour and iron removal. However, the substructure morphology (regularly spaced micro-voids) made the membranes susceptible to fatigue and breakage. Although it is a simple operation to remove a substandard module from a membrane plant, identify and repair individual compromised membranes, and put the

---

[v] Lmh refers to membrane flux and is an abbreviation for: litres of filtrate produced per square metre of membrane area per hour.

[§] PEG is an abbreviation for poly(ethylene glycol), a linear flexible water-soluble polymer, used to determine the molecular mass cut-off of an ultrafiltration membrane.

module back into service, one would rather make use of a membrane that is mechanically more robust. In addition, a membrane with a lower molecular mass cut-off would remove greater proportions of natural organic materials and other smaller species present in surface streams. It is for these reasons that the development of a new capillary membrane with a lower molecular mass cut-off was attempted.

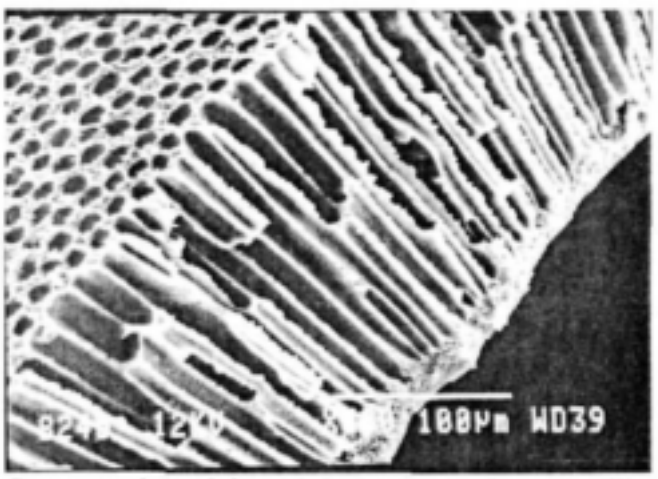

Cross-section of the skinless polysulphone capillary membrane.

Ultrafiltration membranes with various morphologies are available on the commercial market. The morphological properties of these membranes are summarised in the table below.

Morphological properties of ultrafiltration membranes

	Type 1	Type 2	Type 3	Type 4	Type 5
Internal surface	Ultra-skinned	Ultra-skinned	Ultra-skinned	Ultra-skinned	Ultra-skinned
Substructure	Microvoids	Microvoids	Spongelike	Spongelike	Microvoids
External surface	Not skinned	Ultra-skinned	Micro-skinned	Ultra-skinned	Micro-skinned

The skinless membrane, which is operated from the inside-out, falls in the Type 1 category, and is only produced in RSA. Membranes with Type 2 morphology were introduced in Japan in the early 1990s, and were promoted as double-skinned membranes. The rationale behind the development of this membrane was that the double skin would pose as a double barrier to the passage of pathogenic organisms.

One of the tasks undertaken in this project was to develop a lower molecular mass cut-off membrane than the one shown earlier, but with a Type 3 or Type 5 structure. It was furthermore argued that a membrane with a Type 3 structure would be mechanically stronger than one with a Type 1 structure. Initial performance aims set for the membranes under development were:

- instantaneous burst-pressure: >1.5 MPa;
- specific pure-water flux: >1.5 Lmh/kPa; and
- PEG35000 molecular mass cut-off: >90%.

Further to the development of a Type 3 structured polysulphone membrane that has a spongelike substructure and a microfiltration-type outer skin layer, attempts were also made to develop a Type 5 poly(ether sulphone) membrane, which has a substructure similar to the structure shown earlier. However, in the case of this membrane the membrane has a microfiltration-type skin layer on the outside as apposed to being unskinned as is the case with Type 1 membranes. The external skin of the Type 5 membranes should add to the mechanical integrity of the membrane, whereas the presence of the microvoids in the substructure should decrease the resistance to fluid transport.

The tables below show some results obtained during the development of the poly(ether sulphone) and polysulphone membranes respectively. The substructure morphology of the polysulphone membrane that was developed is shown in the figure below.

Performance of the initial poly(ether sulphone) membranes (Type 5 morphology)

Code	PWF 100kPa (Lmh)	Ultrafiltration flux (Lmh)*	Ultrafiltration retention (%)	Burst-pressure (kPa)
P04/98	130	52	72	1 600
P05/98	128	48	68	1 600
P06/98	135	60	66	1 600

Ultrafiltration test: 0.2mm²ₐ 35000 PEG, 100kPa, 0.5m/s velocity

Performance of polysulphone membranes (Type 3 morphology)

Production code	9902	9904	9909	9911	9914	9917
PWF (Lmh) (100kPa)	134	148	147	137	126	114
UF flux (Lmh) PEG35000 100kPa	56	38	38	34	39	31
Retention (%)	92	97	91	91	95	92
Burst-pressure (kPa)	1 800	2 100	1 850	2 200	2 050	2 200
Bubble pressure (kPa)	200	250	250	250	300	250

The MMCO test is performed with PEG35K at a feed concentration of 0,5% by mass as opposed to 0,25mm.

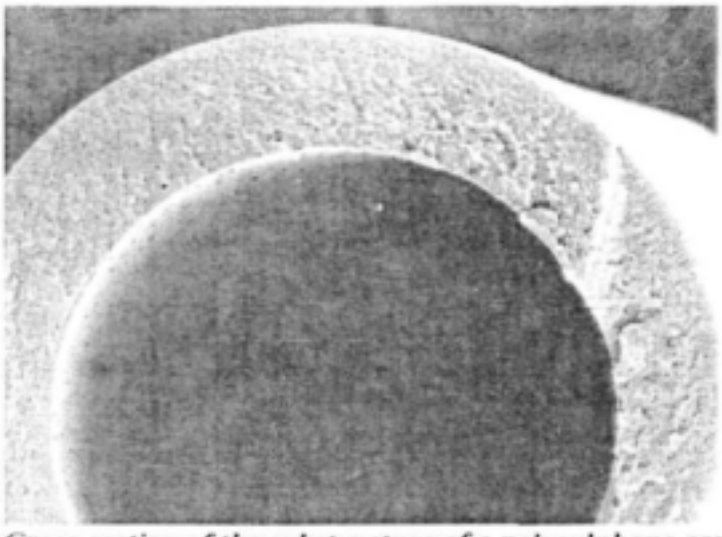

Cross-section of the substructure of a polysulphone capillary membrane.

Membrane modification

The aim of this work was to develop a technique whereby the surface characteristics of a hydrophobic membrane could be modified in order to render it hydrophilic. If the surface of a membrane could be hydrophilised, membrane fouling would be reduced and flux performance increased. Hydrohilisation will not prevent the formation of concentration polarisation gel layers on the membrane surface, but it will prevent such layers to associate with the membrane as result of hydrophobic interaction. Reduced fouling will lead to longer filtration runs and less frequent chemical cleaning.

A commercially available non-ionic tri-block copolymer surfactant was used as a first approach. The choice fell on Pluronic® F108 (Pluronic), a material known to adsorb readily onto hydrophobic membranes. Pluronic is a tri-block co-polymer of poly(ethylene oxide) (PEO) and poly(propylene oxide) (PPO). This material is non-toxic and non-invasive.

The Pluronic range of materials is classified as surfactants and the material used is synthesised to have the following block form: $-(PEO)_n-(PPO)_m-(PEO)_n-$. In a polar solvent environment such as water, the hydrophobic middle block $(PPO)_m$ will adsorb onto hydrophobic surfaces. The PEO segment has no particular affinity for the hydrophobic interface and will tend to float free in the solvent. This will impart some hydrophilicity to the surface of a hydrophobic membrane and reduce adsorptive fouling. Earlier work by the group showed that membranes treated with Pluronic and subsequently fouled with paper and pulp effluent responded much better to chemical cleaning than membranes did that was not treated with the Pluronic. However, loss of initial flux was observed when the membranes were coated with the Pluronic material grade used. It was argued at the time that the resistance caused by footprint of the adsorbed hydrophobic segment of the surfactant gave rise to restricted permeate flow. This problem would not be overcome simply by substituting the hydroxyl end-groups of Pluronic with charged moieties.

Still within the framework of the project aims, however, another embodiment of the surface-coating approach would be for the adsorptive coating material to act as a linker and tether onto which an enzyme could be covalently bonded. This modified material could be used to effect bioconversion in a membrane reactor application. This would be a much less expensive approach than to attach reactive tethers onto the membrane material prior to membrane manufacture or to graft such tethers onto the surfaces of membranes after fabrication.

With the certainty that Pluronic does indeed have an affinity for the membrane, the question was whether one could replace the hydroxyl end-groups of the macromolecule with some other moiety to advantage. Two possibilities offered themselves. If one were to replace the hydroxyl groups with an amine, one could attach an enzyme covalently to the Pluronic via the amine functionality. This could be used to benefit bioconversion in a membrane bioreactor application.

The second possibility was to attach a ligand to the Pluronic, either by way of the aminated end-groups, or by ion exchange end-group functionality. In the latter case, the hydroxyl groups of the Pluronic material would have to be replaced with either quaternary ammonium salts or sulphonic acid groups. If this can be achieved, it offers the possibility to use this technology as a down-stream operation to recover enzymes produced in a gradostat bioreactor, for example.

It was decided to opt for the affinity separation route to prove the hypothesis because of its relative simplicity, rather than to immobilise enzymes in this fashion and rely on rate of conversion of tether versus surface immobilised enzymes to compare relative efficiencies of these two methods of immobilisation.

To allow covalent coupling of a ligand to the Pluronic material, the hydroxyl end-groups on the poly(ethylene oxide) chain had first to be converted to an amine moiety. This was successfully achieved and techniques to purify the reaction mixture were devised. Cibacron Blue 3GA was subsequently coupled to the amine-Pluronic material and purified by chromatography. The Cibacron Blue 3GA ligand has an affinity for albumin. The next step was to adsorb the ligand-carrier onto polysulphone capillary membranes to effect an affinity matrix. A test cell containing a large amount of coated membranes was subjected to a feed of sheep serum. Subsequent elution of the matrix with an appropriate buffer solution stripped the adsorbed sheep serum albumin from the column. The SDS-PAGE slide on the next page indicates to what extent pure sheep serum albumin was stripped from the sheep serum solution.

The fraction in lane 9, eluted from the affinity matrix, showed only a single band corresponding to the serum albumin in lanes 6 and 7. It is apparent from the results that sheep serum albumin could indeed be separated effectively from the other serum proteins using the affinity matrix developed. The degree of purification is seen when the content of lanes 1 to 4 is compared with lane 9.

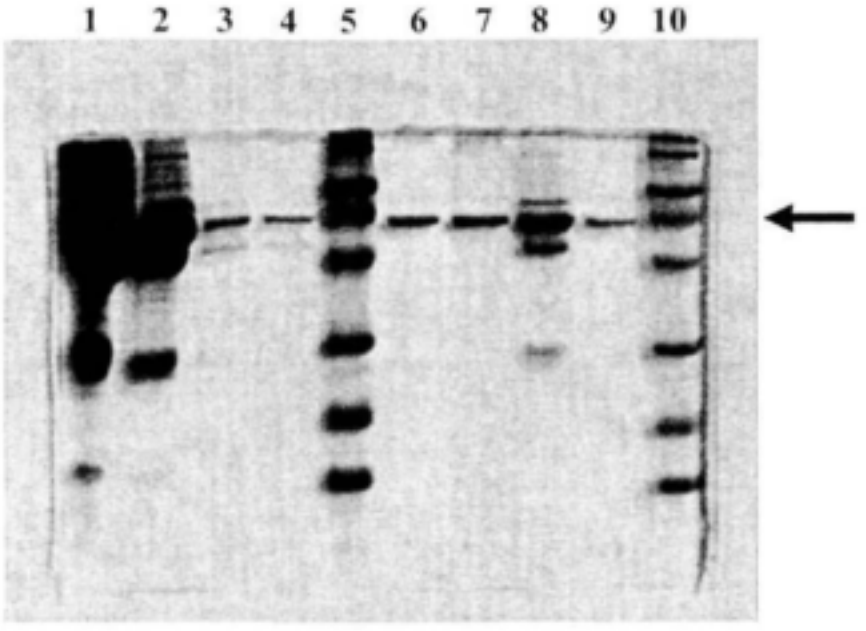

Axial-flow module and manifold development

The focus on module development gravitated to the development of more effective and inexpensive axial flow modules. Various lines of thought were followed and evaluated concerning alternative designs for the module (scale-up of filtration area, materials of construction, cost, etc) and the manifolding system.

The 90°mm membrane cartridges were manufactured to slide-fit into the side-branch of standard u-PVC T-pieces. The manifold consists of individual T-pieces that are either flanged or solvent-welded together to form the manifold. The modules are provided with two O-rings, which offer the hydraulic seal between the 110mm tube-sheet on the module and the side-branch of 110mm u-PVC T-pieces. The downside of this simple technique to create a filtration loop was that the top and bottom manifolds needed to be kept in place with cable stays to prevent them from telescoping under pressure. This made the removal of individual modules not a trivial task, especially not if the modules were in operation for a few months and the O-rings had *frozen* in place. The photograph below shows an example of the 90mm module manifold and cable stays.

After much deliberation and experimentation, the clamping and manifold system was adapted, taking cost and ease of module removal into account. During the time a computation fluid dynamic exercise was conducted to establish appropriate module sizes, because one of the aims of the project was to up-scale the 90mm module to enlarge the filtration area per module.

A simple method to secure modules to a manifold is by way of flanges. The technique eventually adopted was to cast a flange onto the module as part of the membrane tube-sheet. The potting compound used in the construction of the 90mm modules was not adequate for the new module fabrication approach and a new formulation had to be developed. This was achieved and the flanged-type modules

were pressure tested up to 5bar for weeks to establish mechanical integrity of the securing technique. The difference between the 90mm and 110mm module connectors are shown in the photographs below.

Bayonet-type 90 mm module

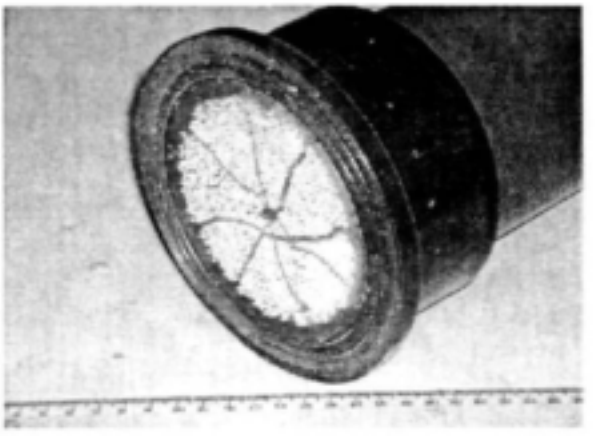

Flange-type 110 mm module

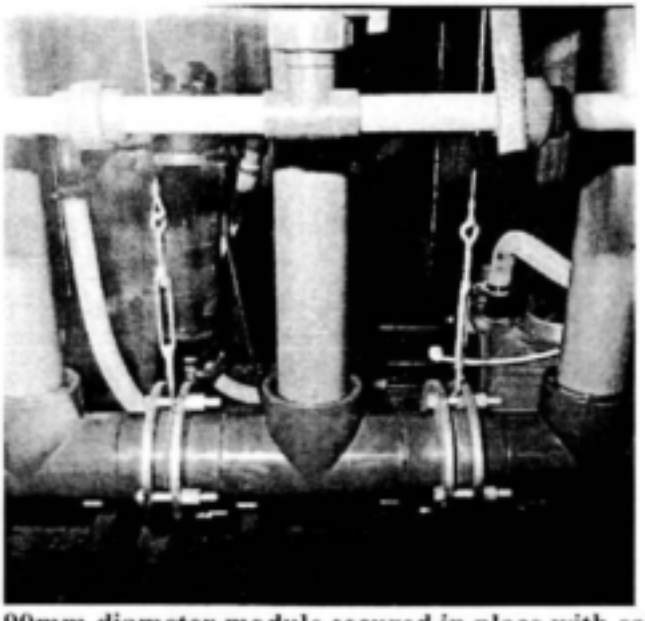

90mm diameter module secured in place with cable stays, the manifold being bolted together with flange clamps.

The computational fluid dynamics modelling work suggested that 200 mm diameter modules would be a sensible scale-up size of a capillary membrane module. Such a module would contain 23 m^2 filtration area, which is more than 4-times the area contained within a 90 mm module. The photograph below shows the prototype module developed. The flange was tested at 1 MPa pressure for a number of weeks without problem. Bearing in mind that the operating pressure of capillary

ultrafiltration membranes are rarely above 2 bar, the safely margin is adequate to ensure long-term operability.

Modules need to be manifolded to incorporate the filters in the hydraulic filtration loop. Various techniques and designs were evaluated to construct sensible and cost-effective manifolds. Two techniques were devised. In the one approach use is made of 110 mm T-pieces onto which machined standard stubs are hot-melt welded. This will become the standard manifold design for 110 mm modules. This method, however, is not cost-effective for the 200 mm modules, given the cost of injection-moulded T-pieces. In this case a manifold was devised that consists of the main manifold (200 mm straight PVC pipe), onto which reducers are hot-melt welded. A machined serrated stub is in turn hot-melt welded onto the reducer. In this way a relatively inexpensive manifold can be created. A photograph of the 200 mm stainless steel shrouded module is shown below, followed by a diagram of the manifolds developed for the 110 mm modules.

200 mm, 23 m^2 stainless steel shrouded capillary membrane module.

Conclusions

Membrane development

A new polysulphone membrane with a spongy substructure was successfully developed and tested in the field. This membrane had superior mechanical properties to that of the skinless membrane, which it superseded in potable water production applications. The membrane was extensively tested in the field.

A double-skinned poly(ether sulphone) membrane with a void-like substructure was also developed and evaluated in the field. No problems were incurred during field trials of the new membrane.

Mixing within spinneret flow passages can be improved by introducing shear planes to prevent spin-solution channelling within tube-in-tube spinnerets.

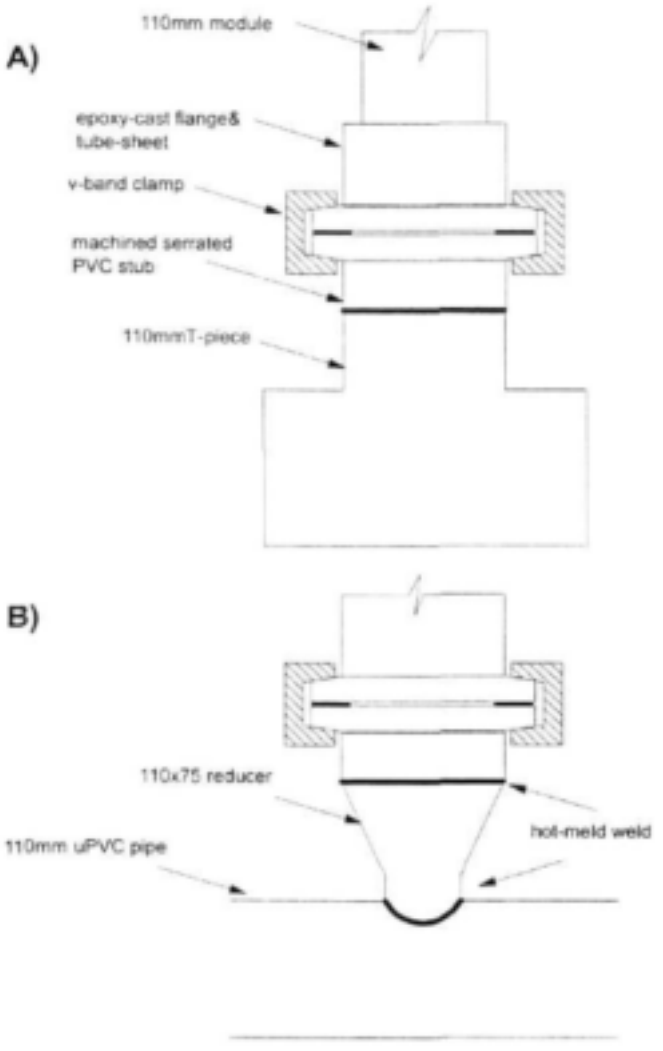

Techniques devised to manifold 110mm modules. Representation (B) being the preferred for 200mm modules.

Membrane modification

Coating the membranes with Pluronic, a tri-block copolymer, non-ionic surfactant can alter the flux and cleaning properties of polysulphone membranes. No binding of proteins occurred if the membranes were coated with Pluronic. However, because of the low fluxes achieved with membranes coated with Pluronic, this approach to membrane performance enhancement was terminated.

As an alternative, the coating material was used as a mediator to effect other properties to a membrane. The suggestion to alter the Pluronic by covalent attachment of a ligand was researched in a successful study on the isolation of sheep serum albumin from sheep serum. This provided the necessary proof that the hypothesis of an adsorptive-carrier, mediating affinity separation, cannot be rejected.

Cibacron Blue 3GA (a ligand for albumin) was covalently coupled to Pluronic after the hydroxyl end-groups of the poly(ethylene oxide) side chains were first converted to primary amines. Polysulphone membranes were coated with the ligand-carrying Pluronic, yielding a polysulphone affinity matrix. The preliminary isolation of sheep serum albumin from sheep serum was first carried out on a single fibre CBAP-PSf matrix to test the efficiency of the method. The work was concluded on a multi-fibre CBAP-PSf matrix. The results obtained with the multi-fibre system indicated that the technique could be used in preparative separations.

Manifold and axial-flow capillary module development

From the stand of simplicity of fabrication, which is also a function of cost, a shell-and-tube axial flow module configuration was chosen as the standard design.

The CFD results indicated that there is some justification in choosing 110mm and 200mm shroud sizes as standard to house capillary membranes. These modules will respectively contain 7 and 23m^2 membrane filtration area. The eventual choice of shroud material was based on cost and reusability of the shroud material; 110mm u-PVC and 200mm welded stainless steel sheet.

In order to save on capital and operational cost for small membrane systems, it is anticipated that the ability to perform chemical cleaning *in situ* may not be engineered into small systems' design. For that reason it is essential that modules can be removed and replaced without much effort. Flanged-type coupling of modules to manifolds is therefore favoured, as opposed to the bayonet designs originally developed for the 90mm modules.

Technology transfer

Applied research outputs

The project started in 1997 and was extended until 2001, without additional funding, in order to meet its objectives with respect to module scale-up, one of the main aims of the project. This has been achieved and larger-sized modules were made available to WRC Project K5/965 and K5/1070 for field evaluation.

The membranes that were developed, notably a polysulphone ultrafiltration membrane with a sponge-like substructure and a double-skinned poly(ether sulphone) membrane were tested extensively in the field by WRC Projects K5/965 and K5/1070. The membranes were also evaluated by WRC Project K5/1034 to establish microbiological retention performance criteria. These membranes are essentially available for commercial exploitation.

The manifolding systems devised during the project work well and are simple to construct without expensive tooling. These manifolds are now also available for commercial use.

The affinity separation technology initiated in this program is being researched further in a WRC project K5/1165, where different ligand systems are being developed for various applications in the water industry. Notably, is the development of an affinity separation based technique as a tool for the rapid detection of endocrine disruptive chemicals in water.

The project identified the usefulness of surface-coating as a means to prevent non-specific binding of species onto hydrophobic membrane materials. The commercial material tested did not render the results anticipated. However, the idea is sound and the membrane coating-approach to induce membrane hydrophilicity is the subject of study of WRC project K5/1248.

Capacity building

The project acted as a hub for many WRC related and other projects that involved membranes, especially capillary membranes. Students of colour from other institutions, notably Peninsula Technikon, Cape Technikon and ML Sultan Technikon were introduced to techniques developed in our laboratories on a very regular basis. These included membrane making procedures, construction of test cells and methods used to evaluate low-pressure operating membranes.

In-service-training students (chemical engineering and analytical chemists) from Peninsula Technikon, funded through an ESKOM TESP project, also worked as assistants on the project since its inception and in doing so, were schooled in the finer points of membrane technology research and development. All these students continued and completed their studies at B-Tech level. Unfortunately, none of the

Cape-based students that were involved with the project continued their studies at M-Tech level.

Two students (PhD – Polymer Science, M Eng – Chemical Engineering) worked on aspects of the work for higher education. The rest of the development work was shared between project staff and in-service-training students from Peninsula Technikon.

Dissemination of results

The basis of the work in this project was to gear and upgrade artefacts from previous WRC projects for commercial exploitation. Not much of the results emanating from the project were submitted for publication in journals yet. Below is the list of publications that did result.

Submitted

- C Yaniç, EP Jacobs, MW Bredenkamp, P Swart and LE Liebenberg, A new approach to membrane-based affinity separation. (I) Serum albumin isolation as model, J of Chromatography, (April 2001).

Published

- C Yaniç, MW Bredenkamp, EP Jacobs, HSC Spies and P Swart, NMR Spectroscopy as basis for the characterisation of Pluronic® F108 and its derivatives, J of Applied Polymer Science, 78(2000)109-117.

Conference proceedings

- Membrane-based affinity separation matrices for the isolation of value added products from biological effluents: Dollars or Dreams? C Yanic, MW Bredenkamp, EP Jacobs and P Swart, 21 Century International Symposium on Membrane Technology & Environmental Protection, 18-21 September 2000, Beijing, China.
- Non-covalent modification of polysulphone membrane surfaces for affinity separation, C Yanic, MW Bredenkamp, EP Jacobs and P Swart, BiotechSA2000 Conference, 23-28 January 2000, Grahamstown.
- Chemical modifications on water soluble polymers, MW Bredenkamp, EP Jacobs, P Swart and C Yanic, 7th International Chemistry Conference in Africa, 34th Convention of the SA Chemical Institute, 6-7 July 1998, University of Natal, Durban.
- Membrane-based affinity separation matrices for the isolation of value added products from biological effluents, C Yanic, MW Bredenkamp, EP Jacobs and P Swart, WISA2000 Biennial Conference, 28 May – 1 June 2000, Sun City.
- The hydrodynamic characterisation of an axial-flow membrane module, SM Bradshaw, EP Jacobs and PC Marais, 3rd WISA-MTD Workshop, 26 – 29 September 1999, Drakensville Resort, Natal.

- Polymer end-group modification for affinity separation, C Yanic, P Swart, EP Jacobs and MW Bredenkamp, 3rd WISA-MTD Workshop, 26 – 29 September 1999, Drakensville Resort, Natal.

Recommendations

It is recommended that consideration be given to the following areas of research:

Membrane development

Consideration should be given to the development of high molecular mass cut-off membranes as well as microfiltration membranes. These membranes will provide greater flux performance and are suited for use in potable water provision where colour, iron and aluminium removal is not required.

Consideration should also be given to develop ultrafiltration and/or microfiltration membranes from hydrophilised hydrophobic materials. Such membranes will have the chemical and oxidative stability inherent of hydrophobic materials, combined with a lower fouling capacity.

Membrane bioreactors

Membrane bioreactors find increasing application in industrial and domestic wastewater treatment. Consideration should be given to the development of membrane modules that are suitable for use in membrane bioreactor applications. The development of narrow-bore high-flux capillary membranes and flat-sheet membranes and manifolding systems to house the membranes should form part of such a research effort.

Process development

Affinity separation is an attractive approach to remove specific biologically active compounds from a mixture. Consideration should be given to investigate the usefulness of the approach developed during the course of the project for the detection of endocrine disruptive chemicals in water sources.

Commercialisation

Some of the products developed during the course of the project are ready for commercialisation. Consideration should be given to make the technology available for commercial exploitation.

-oooo00O00oooo-

Fabrication and production protocol for capillary ultrafiltration membranes and modules

List of Figures

Nomenclature

$\underline{1}$	unit vector
A	membrane surface area, m^2
A_{flow}	cross sectional flow area, m^2
A_v	membrane surface area per unit volume available for fluid
B_1, B_3	transport, m^2
C	constants in eqs. 10, 15, 16
E	constant in eq. 19
k	power consumption, kW
L	Darcy permeability, m^2
L_p	permeable length of dry fibre, m
$L_{p,app}$	membrane permeability, m
L_{wet}	apparent membrane permeability, m
N	permeable length of wet fibre, m
P	number of fibres
Q	pressure, Pa
r	volumetric flow rate, m^3/s
r_L	radial position, m
r_M	fibre inner radius, m
r_S	fibre outer radius, m
u	Krogh cylinder radius, m
$\underline{V}$	axial superficial velocity, m/s
x	superficial velocity vector, m/s
	axial position, m

Greek letters

α	dimensionless parameter
ϕ	fluid source/sink, s^{-1}
γ	dimensionless parameter
η	pump efficiency
κ	dimensionless membrane permeability
λ	dimensionless parameter
	fluid viscosity, Pa.s

μ

Abbreviations

CCF	**Capital Charge Factor, year^{-1}**
ID	**inner diameter, mm**
KCM	**Krogh Cylinder Model**
OD	**outer diameter, mm**
PMM	**Porous Medium Model**

Subscripts

L	**lumen**
r	**radial**
S	**shell**
x	**axial**

1.0 Introduction

Capillary membranes are narrow-bore tubelike membranes. These membranes are self-supporting, that is, their construction is such that they can withstand pressurisation from within or from the outside without bursting or collapsing. Typical operating pressures of these ultrafiltration or microfiltration membranes are below 2 bar. Because the membranes are self-supporting, it is possible to reverse the direction of flow across the wall of the membranes by reversing the pressure differential. This effectively allows the membranes to be back-flushed, a process whereby foulants that have accumulated on the membrane surface may be dislodged and rinsed from within the individual membranes and module.

Capillary membranes are also referred to as hollow fibres, a term that we prefer to use for tube-like membranes where the bore diameter is so small that one cannot operate them to filter from the lumen-side out. Typical dimensions of capillary membranes range from inside diameters as small as 0.9 mm up to 3 mm. As the diameter of the membranes increases the burst-pressure limits decreases. That places some restriction on the operating pressure limits of these membranes.

As a rule of thumb, capillary membranes should not used on a feed water where particles present in the water is greater than 10% of the internal diameter of the membranes. This is to prevent clogging of the membrane entrances by particulate species present in the feed water. The membranes that were developed during earlier research projects had internal diameters in the region of 1.2 mm, suitable for process water that underwent limited pre-treatment. Bearing in mind that this technology was aimed for use in potable water production, this dimension would be suitable for use in an application where the minimum feed pre-treatment required is that of sand filtration.

At the start of the project the knowledge to produce skinless ultrafiltration membranes from polysulphone was in place (WRC project 632). Knowledge also existed to construct 90 mm modules (5 m^2 membrane area) to house the membranes for use. However, further improvement of both the membrane and module was deemed necessary before the technology could be regarded acceptable for application and commercialisation.

The objectives set for this project were in essence therefore formulated in order to further the capillary membrane technology that existed towards application and commercial acceptance.

The original aims of the project, as set out in the research contract, can be subdivided into three categories. These, as well as the individual aims, are listed below.

Capillary membrane production development

- Devise a fabrication protocol to produce capillary membranes with enhanced separation properties for use in water filtration and extractive adsorption of contaminants in aqueous streams.

- Develop a fabrication protocol to produce capillary membranes with special functionality to enable enzymes to be immobilised in a membrane bioreactor for the treatment of aqueous effluent or other product/process stream.

Membrane modification

- Expand the range of neutral surface adsorptive coating materials to include materials with cationic or anionic moieties.

- Devise a simple protocol to modify the surface chemistry of operational membranes by adsorptive techniques to improve their anti-fouling characteristics and operating flux.

- Integrate membrane surface modification with cleaning protocol and determine the efficacy of such a combined approach in difficult applications.

Axial-flow module and manifold development

- Improve and scale-up the design of prototype and semi-production 50 m^2 axial-flow capillary membrane modules for use in low-cost treatment operations.

- Improve and scale up the design of prototype and semi-production transverse flow modules to capitalise on the greater back-mixing properties of this type of membrane device.

Research was initiated during the course of the project to test the integrity of both membranes and modules that were developed during this project. For that reason the project was closely aligned with WRC projects K5/965 (*Capillary ultrafiltration membrane process and systems R&D)*, K5/1070 *(The development of small-system ultrafiltration systems for potable water production)* and K5/1034 (*Microbiological performance criteria for membrane technology for wastewater treatment*) towards the end of the project.

These above-mentioned projects were ideally positioned to offer feedback on the quality and integrity of both membranes and modules, or other shortcomings, should they be detected. This turned out to be a sound approach and much value has been

added through consideration being given to feedback received from workers involved with the above-mentioned projects.

The report is divided into chapters, each chapter referring to the objectives under the above main headings. Chapter 2 reflects on aspects pertaining to membrane development and Chapter 3 addresses membrane modification by means of surface coating. Capillary membrane module development and up-scale are discussed in Chapter 4. These chapters are followed by conclusions and recommendations for further research.

2.0 Capillary membrane production development

2.1 Introduction

Past research focussed on the development of an outer skinless polysulphone membrane. This specially developed membrane is now used in studies on the continuous production of enzymes by filamentous fungi in a membrane bioreactor application. The low-pressure membrane that resulted had very high specific-flux values, typically 2 to 4 Lmh/kPa, and PEG35000 molecular mass cut-off values of less than 80%.

The skinless membrane was also extensively used in the laboratory in various applications and in field evaluations for potable water production. The membranes performed well in potable water production applications, especially concerning colour and iron removal. However, the membrane substructure morphology (regularly spaced micro-voids) made the membranes susceptible to fatigue and breakage (Figure 1). The membrane is also difficult to produce reproducibly.

It has proved a simple operation to identify and remove a substandard module from a filtration loop. It is also easy to identify and repair individually compromised membranes in such a module and put the module back into service. However, one would rather make use of a membrane that is mechanically more robust. In addition, a membrane with a lower molecular mass cut-off than that of the skinless membrane would remove greater proportions of natural organic materials and other smaller species present in surface streams.

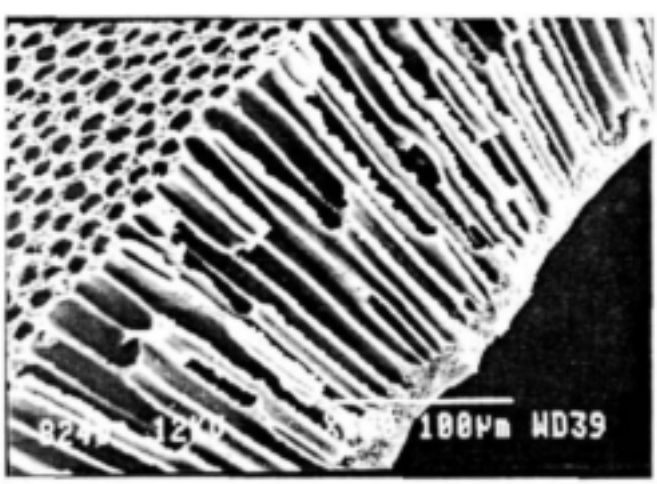

Figure 1: Cross-section of an unskinned capillary membrane, showing the microvoids opening up on the outside of the membrane and the microporous internal skin layer.

Capillary membranes are self-supporting and can operate either being pressurised from the lumen side or from the outside. This is important since it allows the

membranes to be back-flushed. Back-flush, or filtration in the reverse direction, is a very effective and therefore a widely applied technique by which flux is maintained in capillary membrane systems. During the course of another WRC project (K5/965), where systems and process development in a potable water application was studied, a new flux enhancement technique was developed that relied on rapid reverse-pressure swings across the capillary membranes to effect back-flush and flow destabilisation. When the reverse-pressure pulse is introduced, the operating pressure would typically swing from +150 kPa to –70 kPa in less than 2 s. This action places much demand on the mechanical integrity of the membrane. This was a further reason why the development of a new capillary membrane with a lower molecular mass cut-off and better mechanical properties was investigated.

Isotropic and anisotropic ultrafiltration membranes are produced by a phase inversion. During the process a homogeneous solution of the membrane-forming polymer and appropriate solvents is transformed into two liquid phases; the one a polymer-rich phase and the other a solvent-rich or polymer-poor phase. The polymer-rich phase coagulates to form the membrane matrix, whereas the polymer-poor (solvent-rich) phase forms the interconnected porous body within the membrane substructure that eventually opens into the skin layer to give rise to the pores in the membrane skin layer. For the successful formation of an ultrafiltration membrane it should be noted that both these phases must be continuous. A discontinuous polymer-rich phase will generate latex and no membrane will result. A discontinuous solvent-rich phase, on the other hand, will result in a non-porous (dense) membrane substructure that will not permeate water and no useful semi-permeable membrane will result.

Phase-inversion membranes can be formed from any polymer mixture that forms a homogeneous solution under certain conditions of composition and temperature, but which separates into two continuous phases at a different composition and temperature. In the wet phase separation process that is under discussion here, water is principally used as the non-solvent medium to bring about the change in phase.

The morphology of a membrane is essentially affected by adjusting the spinning solution formulation and the subsequent protocol followed to produce the membrane. Many other factors fine-tune the ultimate structure of a membrane, but although important, they play a lesser role than the above-mentioned two.

2.2 Membrane formation

2.2.1 Theory

The thermodynamic state of a membrane system with more than one component and limiting miscibility may be described in terms of free energy of mixing. At constant pressure and temperature, three states exist:

- $\Delta G > 0$ (P, T = constant)
  A positive free energy of mixing – all components are stable and miscible in one phase.

- $\Delta G = 0$ (P, T = constant)
  An equilibrium state represented by the composition at the phase boundary.
- $\Delta G = < 0$ (P, T = constant)
  Negative free energy of mixing. This state is associated with the miscibility gap in the ternary phase diagram, and refers to the unstable state in which the homogeneous spinning solution spontaneously separates into a polymer-rich and polymer-poor phase which are then in equilibrium (Figure 2).

Membrane-skin formation generally results from a process of gelation, which occurs the moment the nascent membrane is brought into contact with a strong non-solvent for the polymer, such as water. It is a rapid process. The skin then forms a diffusion barrier to further solvent/non-solvent exchange, and the substructure of the membrane is formed through the much slower process of nucleation and growth of, respectively, polymer-rich and polymer-poor phases.

2.2.2 *Membrane fabrication and formulation*

Three techniques that may be used to spin capillary membranes are shown in Figure 3. In all the cases under discussion the lumenal non-solvent coagulant is in contact with the nascent membrane the moment the extrudate leaves the spinneret. The rate of internal gelation and coagulation is therefore a function of the activity and composition of the internal coagulant that is either water or mixtures of water and other non-solvents or co-solvents.

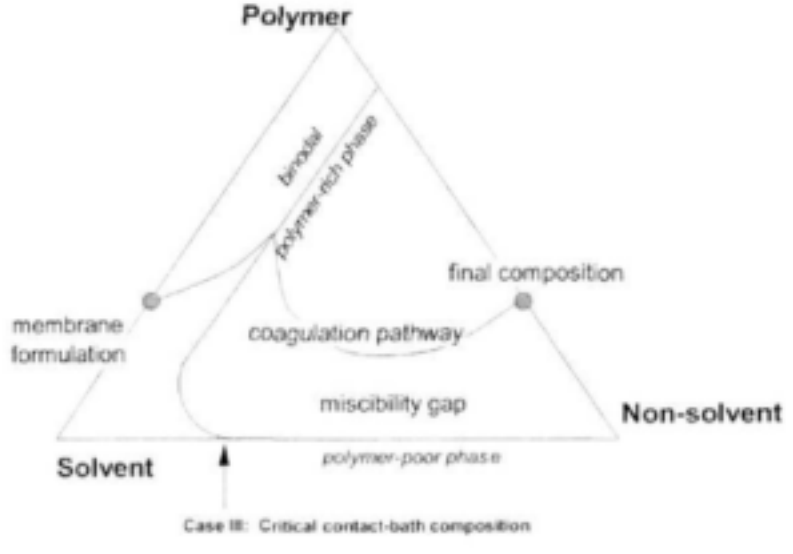

Figure 2: Ternary spinning solution phase diagram.

The three wet phase inversion spinning protocol used during the programme is shown in Figure 3. Cases I and II are known as dry-wet spinning, while Case III is referred to as wet-wet spinning, referring to the condition the nascent membrane encounters the moment it leaves the spinneret.

Case I: The membranes are spun in air at different air-gap distances before they enter into the coagulation bath seconds later. The membrane starts coagulating first from the inside and seconds (or fractions of seconds) later from the outside.

Case II: The membranes are spun vertically downwards through a controlled atmosphere column before they enter into the solvent extraction bath. The membrane essentially coagulates from the outside under controlled conditions.

Case III: The membranes are spun vertically upwards into an aqueous solvent bath, before it is drawn first through a controlled atmosphere column (to fix the phase separated external structure), and then into a non-solvent bath to extract solvents. The membrane coagulates only from the inside.

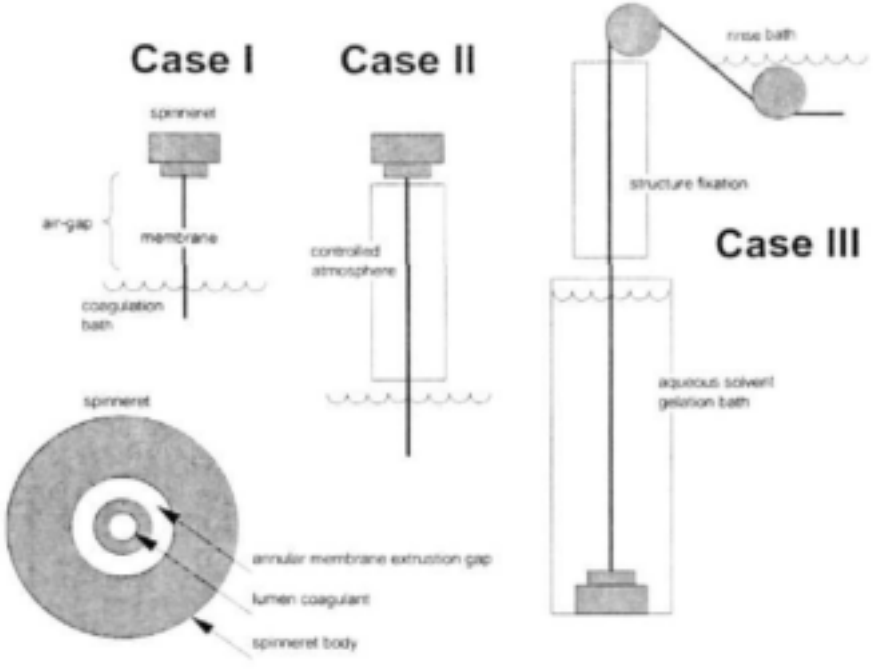

Figure 3: Dry-jet and wet-jet capillary membrane production techniques.

2.2.3 Membrane formation

The membrane solution is spun through a tube-within-tube extrusion die, called a spinneret. The final inside and outside dimensions of the membranes produced during this study were ~1.8 mm and ~1.2 mm respectively, depending on the shrinkage that occurs during the coagulation process or stretching that may be effected during the solvent extraction process. A large number of factors and interactions between factors affect the final morphology of the membranes. A list of the more important factors is given below.

Membrane formulation:

- Membrane-forming polymer material: physico-chemical properties, concentration, molecular mass, molecular mass distribution, etc;
- Solvents, non-solvents and solvent modifiers: physico-chemical properties, concentration, relative concentration ratios, and heat of mixing, etc;
- Non-membrane forming polymer additives: physico-chemical properties, molecular mass, molecular mass distribution, relative concentration ratios, etc; and
- Viscosity and temperature of the spinning dope.

Because of the large number of factors that affect membrane properties, 2-level factorial experimental designs are considered a very handy experimental procedure in membrane development. This experimental technique accommodates not only a study of the effect that main factors have on membrane performance, but also the statistical importance of interactions between factors and their effect on membrane performance.

Fabrication protocol:

- The air-gap (distance between the spinneret and the coagulation bath) and conditions prevailing in the air-gap (solvent and non-solvent vapour pressures, humidity and temperature);
- Temperature and composition of the internal and external coagulation media or contact baths or zones;
- Rate of spinning dope extrusion through the spinneret;
- Temperature, volume-flow and static pressure of the lumen coagulant; and
- Take-up velocity ratio to spinning velocity (membrane stretching to elongate pores in the membrane skin layer).

Provisions:

As mentioned earlier, both polymer-rich and polymer-poor phases must be continuous for the fabricated membrane to be useful for ultrafiltration. Also of importance is that the membrane polymer must be amenable to film-formation, the solvent system and other additives must be miscible with water, and the polymer solution must be homogeneous at the conditions under which the membrane is extruded.

2.3 Low molecular mass cut-off membrane morphology

Membranes with various morphologies are available on the commercial market. Table 1 summarises the typical morphological properties of some of the available membranes.

The skinless membrane mentioned earlier falls in the Type 1 category. The membrane has an ultrafilter-type internal skin, containing microvoids in the

substructure, but with no skin on the outside. The development of this membrane started in a previous WRC programme, although some develop work continued in this project. The Type 1 membranes shown in Figure 1 and Figure 4 are only produced in RSA. As mentioned earlier this membrane is useful in membrane bioreactor and potable water filtration applications.

Table 1: Morphological differences between membranes

	Type 1	Type 2	Type 3	Type 4	Type 5
Internal surface	Ultra-skinned	Ultra-skinned	Ultra-skinned	Ultra-skinned	Ultra-skinned
Substructure	Microvoids	Microvoids	Spongelike	Spongelike	Microvoids
External surface	Not skinned	Ultra-skinned	Micro-skinned	Ultra-skinned	Micro-skinned

Membranes with Type 2 morphologies were introduced in Japan in the early 90s and were promoted as double-skinned membranes. The rationale behind the development of this membrane was that the double-skinned membrane would pose as a double barrier to the passage of pathogenic organisms. Amicon also produces a membrane of this type, although the outer skin layer of their membrane is undulated and not smooth as the Japanese membrane is.

Type 3 membranes are amongst others produced by X-Flow in the Netherlands, whereas membranes with Type 4 morphologies are typical of the membranes that Lyonnaise des Eaux produces.

One of the aims of this programme was to develop a lower molecular mass cut-off membrane than that shown in Figure 1, but with a Type 3 or Type 5 structure. Initial performance aims of these membranes were set at the following:

- instantaneous burst-pressure: >1.5 MPa
- specific pure-water flux: >1.5 Lmh/kPa; and
- PEG35000 molecular mass cut-off: >90%.

Further to the development of a Type 3 structured polysulphone membrane that has a spongelike substructure and a microfiltration-type outer skin layer, attempts were also made to develop a Type 5 poly(ether sulphone) membrane (Table 1), which has a substructure similar to the structure shown in Figures 1 and 4. However, in the case of this membrane the membrane was to have a microfiltration-type skin layer on the outside as apposed to being unskinned, as is the case with Type 1 membranes. The external skin of the Type 5 membranes should add to the mechanical integrity of the membrane, whereas the presence of microvoids in the substructure should decrease the resistance to fluid transport. Furthermore, although the poly(ether sulphone) membranes are less resistant to solvents than their polysulphone counterparts are, the material is slightly less hydrophobic than polysulphone. Membranes fabricated from poly(ether sulphone) should therefore be somewhat less prone to fouling caused by the adsorption of hydrophobic species present in the process water.

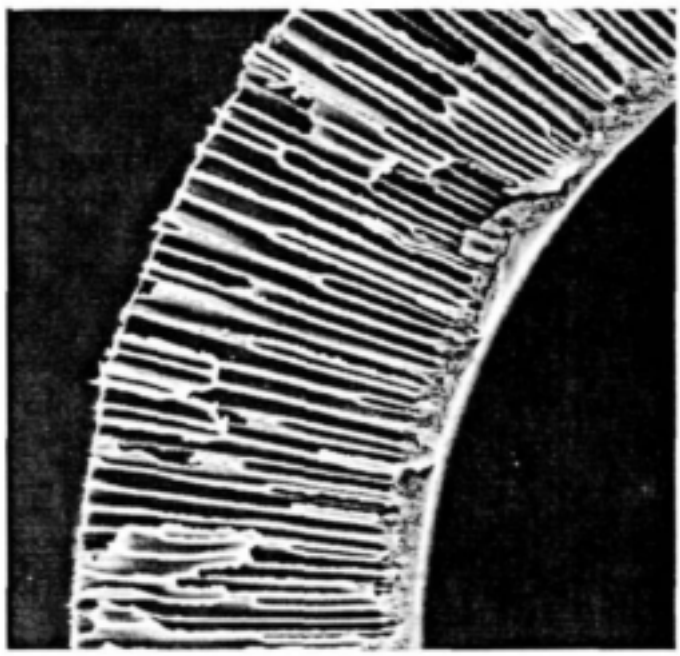

Figure 4: Cross-section of an unskinned Type 1 polysulphone membrane.

2.4 Membrane fabrication

The capillary membranes under discussion are produced by the wet phase inversion technique as mentioned earlier. Although there are variations in how the production techniques are executed, there are essentially only three approaches (Figure 3) that may be followed in the production of capillary membranes, each giving rise to typical membrane morphologies. As was mentioned earlier, the fabrication technique, the membrane material and the membrane formulation all play a role in defining the eventual morphology and performance of the membrane.

There are a number of ways that the formation of microvoids in the substructure of a membrane can be suppressed. One approach is to make use of additives to increase the viscosity of the spinning solution. Poly(vinyl pyrrolidone), a polymer that mixes homogeneously with polysulphone in all proportions is often used as additive for this reason. One manufacturer even makes use of poly(vinyl pyrrolidone) addition to hydrophilise the membrane, making use of an oxidative thermal post-treatment step.

Another approach is to formulate the membrane fairly close to the demixing gap in the ternary phase diagram. Little non-solvent ingress during the precipitation step will lead to the spontaneous formation of polymer-poor nuclei; this is referred to as spinodal decomposition. If spinodal decomposition continues throughout the membrane cross-section, a sponge-like substructure will result. However, microvoids will form at any time after nucleation, if the rate of polymer-poor phase growth exceeds the rate of polymer-poor phase nucleation.

2.5 Spinneret development

When a polymer is dissolved in a strong solvent for the polymer, the polymer chains are relaxed. However, when the polymer is dissolved in lesser strong solvent systems, the polymer tends to coil and form aggregates. This is the case when a spinning solution is formulated close to the phase boundary drawn on a solvent, non-solvent and polymer ternary diagram (Figure 2). The formulation of the sponge-like substructure polysulphone membrane under development in this project falls in this category.

The relatively inexpensive spinneret that was developed in an earlier WRC project worked very well with low and medium viscosity formulations. However, when Type 3 polysulphone membrane formulations were introduced, various problems manifested themselves. The main obstacle to progress was that, because of localised mixing zones within the spinneret, an uneven shear profile was introduced into the nascent membrane as it left the spinneret compression zone (Figure 5). Given that the extruded membrane is exposed to the lumen coagulant the moment it leaves the spinneret, and given that the time for relaxation before coagulation is short and not enough for the mixing energy to dissipate, nucleation kinetics varied along the circumference of the nascent membrane. Liquid-liquid phase separation and not spinodal decomposition was the main phase separation mechanism along the shear planes, resulting in the formation of rows of microvoids along the axis of the otherwise spongelike membrane. When the membrane was over pressurised the membrane would burst along these lines, an obvious unwanted situation.

Much time was devoted to the development of a spinneret to overcome the difficulties experienced with the previous design. As a first approach, various adaptations of the previous spinneret design were experimented with, but although the problem was reduced, it was never completely overcome. The problem with spinneret design is that, although some information is available in open literature, much of the fine-tuning had to be done by experimentation. A new spinneret design resulted from studies into the phenomenon that solved all the problems associated with the previous designs and proved the hypothesis indicated in Figure 5. A typical cross-section of a polysulphone membrane produced with the new spinneret is shown in Figure 6. From this micrograph it is evident that the microvoid-formation problem was solved.

2.6 Membrane characterization

Molecular mass cut-off determination gives some indication of the separation ability of an ultrafiltration membrane. Various macromolecules are used to determine molecular mass cut-off. The more common are polyethylene glycol, dextrans and proteins. Polyethylene glycol is a linear flexible polymer and the least expensive of the mentioned three. The problem with polyethylene glycol is that it is only available up to a molecular mass of 35kD. Dextran, a branched polymer, is expensive, but is available over a very much broader molecular mass range. Proteins are globular species and are available over a very wide molecular mass range. However, it is somewhat more difficult to work with proteins than with the synthetic materials. The gravimetric method used to determine polyethylene glycol and dextran retention is

simple to perform, but it takes some days to evaporate samples to complete dryness at the low temperatures employed.

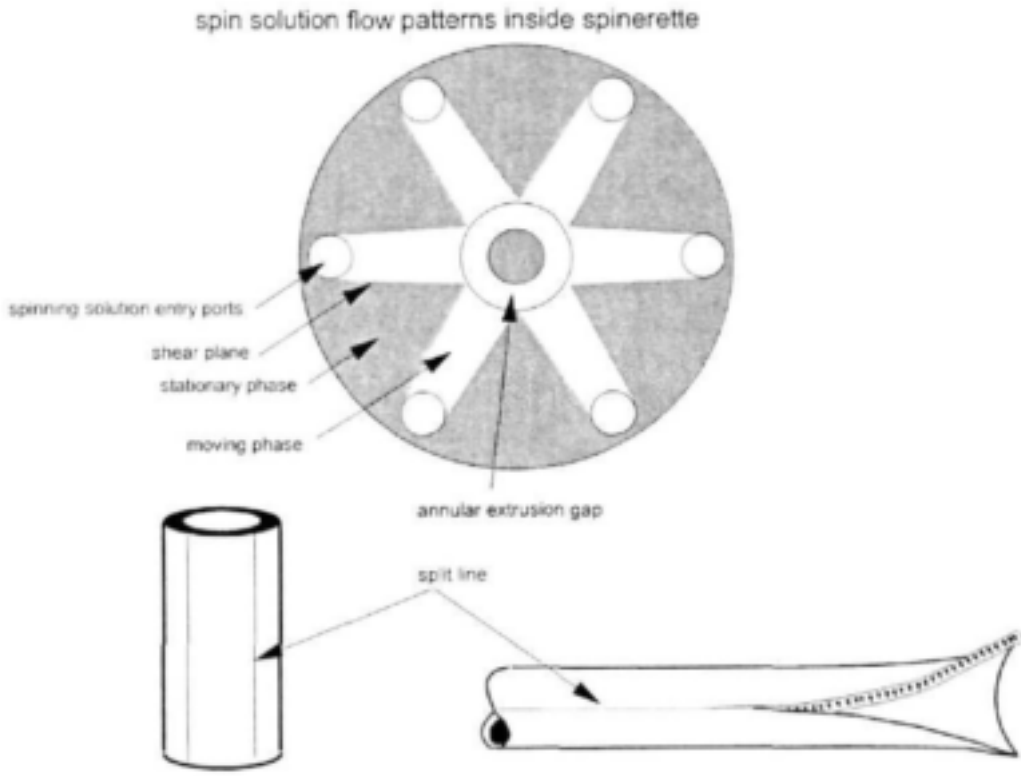

Figure 5: Illustration of the hypothesis to explain the presence of in-line *microvoids that caused longitudinal 'tear lines'*.

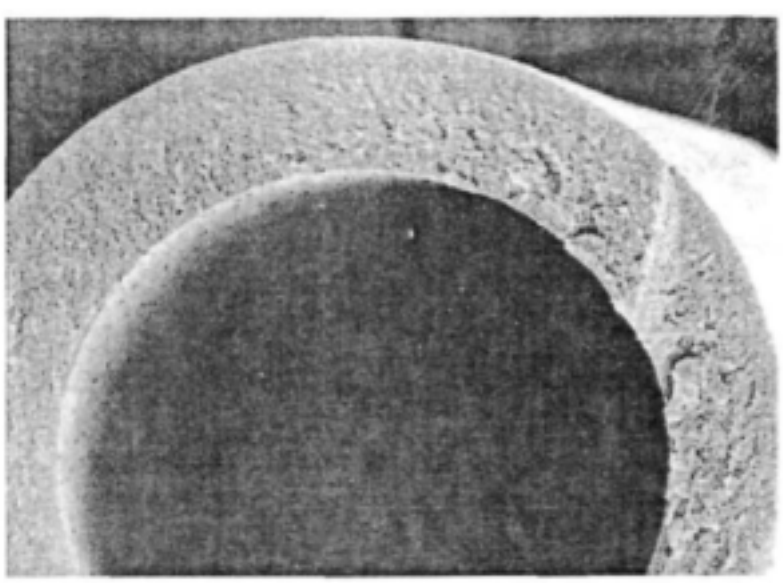

Figure 6: Typical cross-section of a Type 3 polysulphone membrane developed.

Pall Corporation[1] introduced a new and rapid technique by which the molecular mass cut-off of an ultrafiltration membrane can be judged. In accordance with their approach, called the K_{UF} method, the test specimen is completely wetted with a fluid that is capable of wetting the membrane. A displacing fluid, immiscible with the wetting fluid, is placed on the upstream side of the membrane and pressurised. As the pressure is increased, the displacing fluid will force the wetting fluid first from the largest pores, and as the pressure is increased, the displacing fluid will start permeating through decreasingly smaller pores. A plot can be made of the flow rate of the displacing fluid (per unit area of the membrane) through the membrane as a function of the applied pressure. A regression line is drawn through the straight section of the graph that resembles pressure-dependent volumetric flow. The K_{UF} value is read off the intercept of the extrapolated line with the x-axis. A direct relationship exists between molecular mass cut-off, as determined with proteins, and the K_{UF} value.

In this indirect measurement of the molecular mass cut-off of a membrane, 1-butanol, saturated with water, is used as the wetting fluid, and water, saturated with 1-butanol, is used as the displacing fluid. The immiscible phases are mutually saturated to ensure that no interfacial tension exists between the two phases. A simple experimental set-up was constructed to enable the K_{UF} test to be performed. The apparatus consisted of two pressure vessels, a pressure transducer, a three-way valve to switch between the two fluids, the membrane test cell and an electronic balance (Figure 7).

From the K_{UF}-value determined in Figure 8, it appears that the membrane under evaluation had a molecular mass cut-off value of 42kD. This is much higher than that determined by PEG35K (polyethylene glycol) analysis. Some comments may be made when one analyses the data in Figure 8:

- the membrane has a lower flux than the Amicon 50K membrane;
- the pore-size distribution is narrower, evident from the short rise-time between a position of no-flow to pressure-dependent flow; and
- the largest pores in the membrane have a molecular mass cut-off of 52kD.

The K_{UF} test was used as a standard tool to judge and compare the performance of the membranes under development. The technique is also amenable to evaluate membranes taken from the spinning line as a means to quality assurance.

---

[1] Integrity testable wet-dry reversible UF membranes and method for testing same, PJ Degen, J Mischenko, RE Kesting, MH Bilich and TA Staff, US Patent 5 685 991

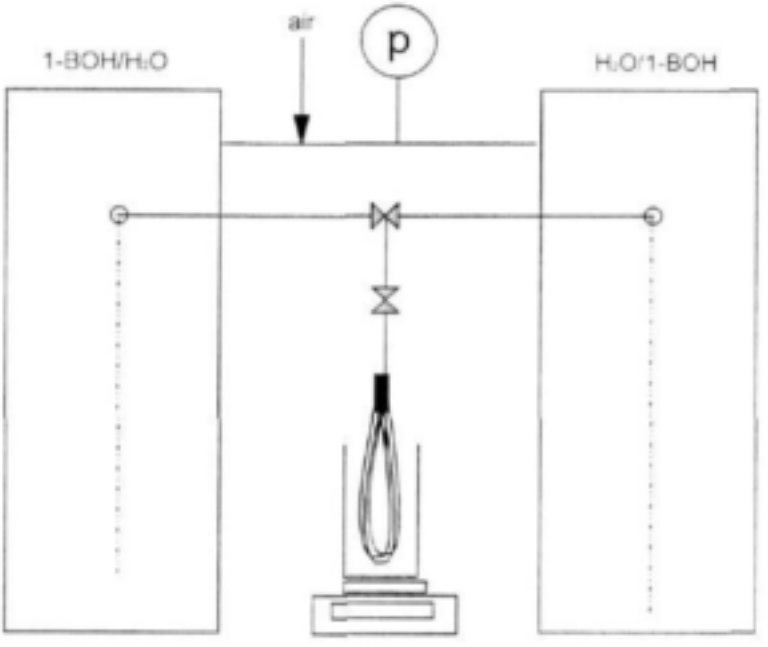

Figure 7: The simple set-up used to perform the K_{LF} molecular mass cut-off test.

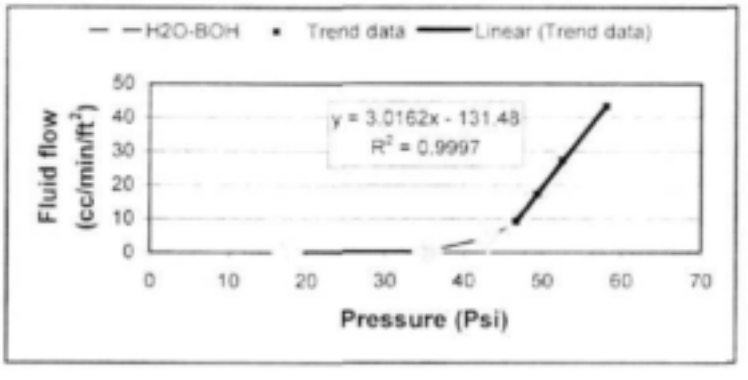

Figure 8: K_{LF} test performed on Type 3 polysulphone capillary membranes.

2.7 Membrane development

Progress has been made with the development of the sponge-like polysulphone membrane. Modules (90 mm double O-ring, 5 m^2 bayonet-type) were constructed with experimental polysulphone membranes and these modules underwent extensive evaluation during field trials. The membranes were also subjected to reverse-pulse cleaning during these trials. No membranes were damaged during the period of evaluation that lasted more than 1 000 h. From Table 2 one can see that the membranes perform reasonably close to the initial performance target set. The next phase of research would be to increase the pure-water flux to values closer to 2 to 2,5 Lmh/kPa, without compromising the retention performance of the membranes.

Table 2: Performance of Type 3 polysulphone membranes

Production code	9902	9904	9909	9911	9914	9917
Pure-water flux (Lmh) (100kPa)	134	148	147	137	126	114
Ultrafiltration flux (Lmh) PEG35000 100kPa	56	38	38	34	39	31
Ultrafiltration retention (%)	92	97	91	91	95	92
Burst-pressure (kPa)	1 800	2 100	1 850	2 200	2 050	2 200
Bubble pressure (kPa)	200	250	250	250	300	250

The molecular mass cut-off test is performed with PEG35K at a feed concentration of 0.5% by mass as opposed to 0.2%mm

Reasonable effort was put into the development of a Type 5 poly(ether sulphone) membrane. This membrane was intended for use in potable water production and immersed membrane bioreactor applications. The solvent and co-solvent system experimented with in the development of the initial membranes did not generate very productive membranes, and a different solvent system was be used in the second round of experiments.

The repeat-unit of polysulphone differs from that of poly(ether sulphone) in that the polysulphone repeat-unit also contains a bis-phenol A moiety. (Typical performance data of the first poly(ether sulphone) membranes produced are shown in Table 3. Although the retention performance data of the membranes is very much less than 95%, which was decided as the molecular mass cut-off benchmark, the consistency in the performance of the membranes produced was encouraging. Towards the end of the project poly(ether sulphone) membranes were produced that had similar pure-water flux and instantaneous burst-pressure performances as the membranes shown in Table 3, but which had 35000PEG retention capabilities that met the 95% benchmark.

Polysulphone is chemically more robust than poly(ether sulphone), but the equilibrium water content of poly(ether sulphone) is slightly higher than that of polysulphone. Based on water droplet contact-angle measurements it may be deducted that poly(ether sulphone) membranes are somewhat more readily wetted by water, which should have a positive effect on reduced adsorptive fouling. However, the difference in chemistry is not such that the membrane will wet out spontaneously and researchers have expended much effort to induce hydrophilicity by chemical intervention.

The research into an ultrafiltration poly(ether sulphone) membrane with an ultrafiltration internal skin layer and a microfiltration outer skin layer demonstrated the difference in chemical composition of the two membrane materials. The three-dimensional solubility parameter of polysulphone and poly(ether sulphone), which takes cohesive energy forces such as hydrogen bonding, dipole interaction and dispersive forces into account, differs slightly and this has an effect on the ternary phase diagram of a polymer/solvent/non-solvent system.

Polysulphone is a resin that is resistant to mineral acids, alkali and salt solutions. Their resistance to detergents and hydrocarbon oils is good, but polar solvents such as ketones, chlorinated hydrocarbons and aromatic hydrocarbons attack polysulphone. The material has a T_g of 185°C. Chemical composition of polysulphone and poly(ether sulphone) repeat units are shown in Figure 9. Poly(ether sulphone), on the other hand, has resistance to boiling water (Tg 220°C) and mineral acids.

It was soon established that it was not difficult to attain the microvoid-type substructure morphology with the poly(ether sulphone) membranes, the problem faced was rather that of permeability. Very unproductive poly(ether sulphone) membranes were initially produced when the same solvent system developed for the polysulphone membranes was used to produce poly(ether sulphone) membranes. It was for this reason that a range of solvent/non-solvent systems were evaluated to map out an experimental window within which 2-level factorial designed experiments could be constructed to improve the formulation and render the membrane more productive. A typical statistical experiment, involving the study of two factors at two levels, is shown in Figure 10. The intention of this particular 2-level factorial experiment was to determine the effect that the addition of a non-membrane forming polymer additive would have on membrane performance. A number of these experiments were conducted to steer the research towards the formulation of a 35 000 kDa molecular mass cut-off (95%) membrane.

A micrograph of the cross-section of the poly(ether sulphone) membrane under development during this phase of the project is shown in Figure 11. Liquid-liquid demixing occurred in the outer section of the membrane shown in Fig11a, hence the formation of microvoids. As development of the membrane progressed (Figure 11b and c), the occurrence of microvoids in the outer region became less predominant. This is because spinodal decomposition became the predominant phase separation mechanism. It is preferred for the outer layer not to have microvoids. The formation of microvoids in the outer region of the membrane was further suppressed as the work progressed (Figure 11d). The morphology of the outer region, however, still need adjustment to reduce the resistance to mass transfer posed by this membrane segment. Ideally the external skin and its support layer should be thin and microporous in order to offer less resistance to fluid transport than the inner skin layer and support structure.

Typical performance data of the first poly(ether sulphone) membranes produced are shown in Table 3. Although the retention performance data of the membranes is very much less than 95%, which was decided as the molecular mass cut-off benchmark, the consistency in the performance of the membranes produced was encouraging. Towards the end of the project poly(ether sulphone) membranes were produced that had similar pure-water flux and instantaneous burst-pressure performances as the polysulphone membranes shown in Table 3, but which had 35000PEG retention capabilities that met the 95% benchmark.

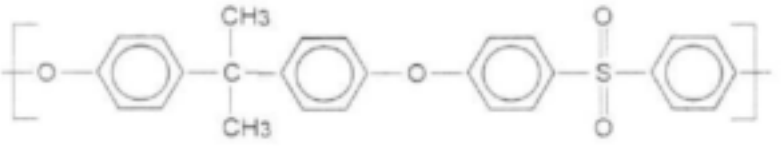

polysulphone

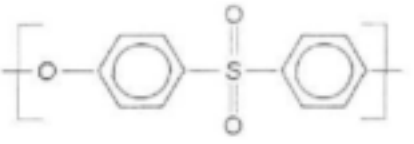

poly(ether sulphone)

Figure 9: Chemical structure of the repeat-unit of polysulphone and poly(ether sulphone) materials.

Table 3: Performance of initial poly(ether sulphone) capillary membranes

Code	PWF 100kPa (Lmh)	Ultrafiltration flux (Lmh)*	Ultrafiltration retention (%)	Burst-pressure (kPa)
P04/98	130	52	72	1 600
P05/98	128	48	68	1 600
P06/98	135	60	66	1 600

Ultrafiltration test: 0.2mm% 35000 PEG, 100kPa, 0.5m/s velocity

2.8 Conclusions

A new polysulphone membrane with a spongy substructure was successfully developed and tested in the field. This membrane had superior mechanical properties to that of the skinless membrane, which it superseded in potable water production applications.

A double-skinned poly(ether sulphone) membrane with a microvoid-like substructure was also developed and evaluated in the field with success.

By adapting the spinneret design to provide even mixing within the spinning solution cavity, the quality of the membranes produced as well as the consistency in performance could be improved.

2^2 Factorial design to determine starting position to optimise PES 35kDa membrane

Mass ratios

Membrane formulation components		Fixed %
Polymer	PES	25
Solvent	NMP	
Non-solvent 1	PA	
Polymer additive 1	Poly I	
Polymer additive 2	Poly II	
Solvent : Polymer / additive mass ratio		3
Relative percent solvent system		75.00
Relative percent polymer additive system		25.00

Factor		-1	0	1
A	mass ratio NMP : PA	8.0	9.0	10.0
B	mass ratio Poly II : Po	1.0	3.0	5.0

Internal coagulant mass ratio	Water	NMP : PA
Ratio	40	1
Mass %	97.56	2.44

Treatment options	A	B
1	-1	-1
a	1	-1
b	-1	1
ab	1	1

Formula number		Internal coagulant formulations (mm%)			
#	1008	*1*	bore-side NMP : PA ratio same as		
#	1009	*a*	the spinning solution NMP : PA ratio		
#	1010	*b*	for each treatment combination		
#	1011	*ab*	Treatm	Water	NMP	PA
#	1012	*0*	*1*	97.56	2.17	0.27
#	1012	*0*	*a*	97.56	2.22	0.22
			b	97.56	2.03	0.41
			ab	97.56	2.22	0.22
			O	97.56	2.20	0.24

1 mass ratio NMP : PA	8.0
Poly II : Poly I	1.0
PES	25.00
NMP	50.00
PA	6.25
Poly II	9.38
Poly I	9.38

a mass ratio NMP : PA	10.0
Poly II : Poly I	1.0
PES	25.00
NMP	51.14
PA	5.11
Poly II	9.38
Poly I	9.38

b mass ratio NMP : PA	8.0
Poly II : Poly I	5.0
PES	25.00
NMP	50.00
PA	6.25
Poly II	15.63
Poly I	3.13

ab mass ratio NMP : PA	10.0
Poly II : Poly I	5.0
PES	25.00
NMP	51.14
PA	5.11
Poly II	15.63
Poly I	3.13

0 mass ratio NMP : PA	9.0
Poly II : Poly I	3.0
PES	25.00
NMP	50.63
PA	5.63
Poly II	14.06
Poly I	4.69

Results

:S	NMP	PA	Poly II	Poly I	Burst pressure	100kPa PEG35 retention	Specific PWF Lmh/kPa
#	50.00	6.25	9.38	9.38	1600	90.65	0.0375
#	51.14	5.11	9.38	9.38	1600	84.35	0.0157
#	50.00	6.25	15.63	3.13	1550	98.5	0.367
#	51.14	5.11	15.63	3.13	1800	99.5	0.17
#	50.63	5.63	14.06	4.69	1500	97.6	0.257
#	50.63	5.63	14.06	4.69	1500	97.4	0.233

Figure 10: Typical layout of a 2-level factorial experimental design.

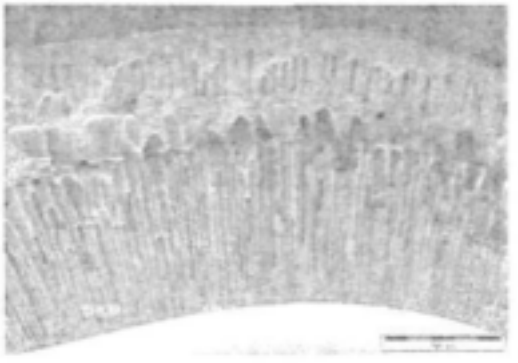

A)

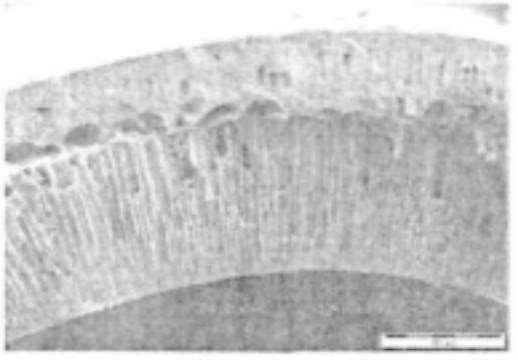

B)

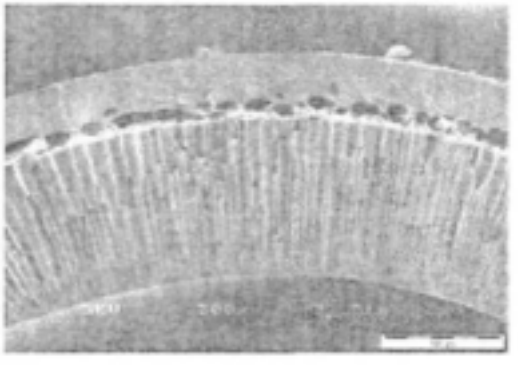

C)

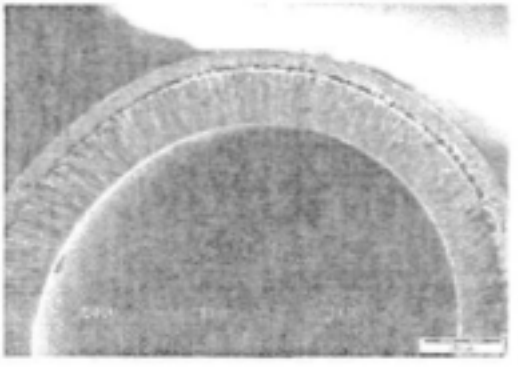

D)

Figure 11: Micrographs showing substructure modification during the development of the poly(ether sulphone) membrane: (A), (B) and (C) 300x magnification; (D) 100x magnification of micrograph (C).

3.0 Membrane modification

3.1 Introduction

The aim of this work was to develop a technique whereby the surface characteristics of a hydrophobic membrane could be modified in order to render it hydrophilic. If the surface of a membrane could be hydrophilised, membrane fouling would be reduced and flux performance increased. Hydrohilisation will not prevent the formation of concentration polarisation layers on the membrane surface, but it will prevent such layers to associate with the membrane as result of hydrophobic interaction. Reduced fouling will lead to longer filtration runs and less frequent chemical cleaning.

A commercially available non-ionic tri-block copolymer surfactant was used first as a coating material. The chosen material, Pluronic® F108 (Pluronic), known to adsorb readily onto hydrophobic surfaces,[2] is a tri-block co-polymer of poly(ethylene oxide) (PEO) and poly(propylene oxide) (PPO). This material is non-toxic and non-invasive.

The Pluronic range of materials is classified as surfactants and the material used is synthesised to have the following block form: $-(PEO)_n-(PPO)_m-(PEO)_n-$. In a polar solvent environment such as water, the hydrophobic middle block $(PPO)_m$ will adsorb onto hydrophobic surfaces. The PEO segment has no particular affinity for the hydrophobic interface and will tend to float free in the polar solvent. This will impart some hydrophilicity to the surface of a hydrophobic membrane and reduce adsorptive fouling. Earlier work by the group showed that membranes treated with Pluronic and subsequently fouled with paper and pulp effluent responded much better to chemical cleaning than membranes did that was not treated with the Pluronic. However, loss of initial flux was observed when the membranes were coated with the Pluronic material grade used. It was argued at the time that the resistance caused by the footprint of the adsorbed hydrophobic segment of the surfactant gave rise to restricted permeate flow. This problem would not be overcome simply by substituting the hydroxyl end-groups of Pluronic with charged moieties.

Still within the framework of the project aims, however, another embodiment of the surface-coating approach would be for the adsorptive coating material to act as a linker and tether onto which an enzyme could be covalently bonded. This modified material could be used to effect bioconversion in a membrane reactor application. This would be a much less expensive approach than to attach reactive tethers onto the membrane material before membrane manufacture or to graft such tethers onto the surfaces of membranes after fabrication.

With the certainty that Pluronic does indeed have a preference to adsorb onto the membrane, the question was whether one could replace the hydroxyl end-groups of

[2] Physical chemistry and process engineering of an emulsion/membrane bioreactor, PhD thesis, Landbouwuniversiteit, Wageningen, Holland, March, 1995.

the macromolecule with some other moiety to advantage. Two possibilities offered themselves.

If one were to replace the hydroxyl groups with an amine, one could attach an enzyme covalently to the Pluronic via the amine functionality. This could be used to benefit bioconversion in a membrane bioreactor application.

The second possibility was to attach a ligand to the Pluronic, either by way of the aminated end-groups, or by ion exchange end-group functionality. In the latter case, the hydroxyl groups of the Pluronic material would have to be replaced with either quaternary ammonium salts or sulphonic acid groups. If this can be achieved, it offers the possibility to use this technology as a down-stream operation to recover enzymes produced in a gradostat bioreactor, for example.

It was decided to opt for the affinity separation route to prove the hypothesis because of its relative simplicity, rather than to immobilise enzymes in this fashion and rely on rate of conversion of tether versus surface immobilised enzymes to compare relative efficiencies of these two enzyme immobilisation methods.

This research was conducted at PhD-level and the results and discussions that will be given in subsequent paragraphs were excerpted or adapted from the thesis.[3]

3.2 Background on affinity separation

Affinity separation is a type of adsorption chromatography in which a molecule is adsorbed specifically and reversibly by a complementary ligand, immobilised on an inert solid support matrix.[4] In principle, affinity separation can be applied where any particular ligand interacts specifically with a biomolecule. For example, specific adsorbents can be used to purify enzymes, antibodies, nucleic acids and vitamins, drugs or hormone binding receptor proteins. Furthermore, the technique can be employed to concentrate dilute protein solutions, separate denatured proteins from biologically active forms of proteins and for the resolution of protein components resulting from specific chemical modifications of purified proteins. This method is superior to other classical means of protein purification.[5]

These affinity separations, as they are currently practiced, typically involve the steps described below:

- a solution containing the compound which is to be separated is passed through a column containing a highly specific ligand (specific for the compound to be separated) immobilised on a solid support;

---

[3] Polymer end-group modification for affinity separation, C Yanić, PhD (Polymer Science) University of Stellenbosch, March 1999.

[4] J N Naval, M Calvo, F Lapreave and A Pinerio, Biochemical Education, 11,1(1983)1-5

[5] CR Lowe, PDG Dean, Chapter 1, Affinity Chromatography, John Wiley & Sons, Ltd., London, 1974, 9-11.

- as the solution passes through the column, the component to be separated binds, both selectively and reversibly to the ligand, while most of the impurities pass through the column unhindered. Any residual impurities are removed by flushing the column with an appropriate buffer solution; and
- the compound, now purified but still bound, is then recovered by passing a solution through the column which disrupts the ligand binding interaction by changing the ionic strength, pH or denaturing.[6]

3.2.1 Ligands and supports

Many types of molecules can serve as ligands, including antibodies, antigens and enzyme inhibitors.[7] The conventional choice of material to support the ligand has been limited to either agarose gel beads or silica particles. Although these expensive systems are quite suitable for affinity separations performed in the laboratory, they are not suitable for use in large-scale separation operations, for amongst others, reasons of cost and scale-up.

In recent years ultrafiltration membranes have been used as support materials for affinity and ion exchange chromatographic protein separation. These membranes have functionalised tethers that are covalently attached to the membrane. This provides an expensive route for ligand attachment. Once the system looses binding capacity, the membrane has to be replaced.[8, 9, 10] The membrane-based chromatographic supports may also have ion-exchange groups to allow selected ligand coupling.[11, 12] Such membranes are referred to as *tentacle type ion-exchangers* and the functional groups are located covalently on polymer chains on the surface of the membrane material.[13, 14, 15]

---

[6] S Brandt, RA Goffe, SB Kessler, JL O'Connor and SE Zale, *Biotechnology*, 6(July)1988)779-782.

[7] P Bailon, DV Weber, RF Keeney, RF Fredericks, JE Smith, C Familletti, PC Smart and JE Smart, *Biotechnology*, 5(1991)45-51.

[8] TB Tennikova, M Bleha, F Svec, TV Almazova and BG Belenkii, *J. Chromatography*, 555(1991)45-51.

[9] M Kim, K Saito and S Furusaki, *J Chromatography*, 585(1991)45-51.

[10] A Higuchi, Y Ishida and T Nakagawa, *Desalination*, 90(1991)1127-136.

[11] P Langlotz and KH Kroner, *J. Chromatography*, 591(1992)107-113.

[12] S Tsuneda, K Saito, S Frusaki and T Sugo, *J. Chromatography*, 689(1995)211-218.

[13] W Muller, *J. Chromatography*, 510(1990)133-140.

[14] S Tsuneda, H Shinano, K Saito and S Furusaki, *Biotechnology Progress*, 10(1994)76-81.

[15] S Matoba, S Tsuneda, K Saito and T Sugo, *Biotechnology*, 13(August) 1995)795-797.

3.3 Outline of the research

The main objective of the affinity separation study was to prove the following hypothesis:

> affinity separation can be accomplished by a ligand, covalently attached to a carrier, where said carrier is immobilised onto a substrate matrix (for the purpose of the study a dense internal skin polysulphone hollow fibre) by forces of adsorption. The carrier has both hydrophilic and hydrophobic functionality and the material selected for use was chosen for the specific ability of its hydrophobic moiety to immobilise itself on a hydrophobic surface by reversible adsorption. In this way, different ligands can be attached to the carrier to effect different separations. The substrate matrix can be reused, because the carrier can be stripped form the polysulphone matrix.

3.4 Experimental approach and discussion

As was mentioned earlier, Pluronic [a tri-block copolymer surfactant of poly(ethylene oxide) and poly(propylene oxide), molecular mass 14 600 Da] was chosen as carrier for ligands. This carrier was chosen because of its specific ability to adsorb onto hydrophobic surfaces, e.g. polysulphone, via the hydrophobic part of the molecule while the hydrophilic end-groups remain for modifications. Pluronic is not commercially available in any form other than the hydroxyl terminated non-ionic form. Hence, the only way in which the carrier could be rendered suitable for covalent attachment of different ligands was to modify the hydroxyl termini into other, more suitable, ionic equivalents. Primary amine equivalents were chosen to obtain a non-ionic carrier. The aminated end-groups would provide sites for covalent attachment of ligands. Sulphonic acid and quaternary ammonium (trimethyl ammonium) bromide end-group modification was also synthesised to provide carriers with ion exchange capacity, but these materials were not experimented with.

The synthetic work was initiated with model compound studies, because it is generally simpler to follow chemical reactions, purify and characterise low molecular mass compounds as opposed to higher molecular mass materials. The model compounds chosen were di(ethylene glycol) methyl ether (DEG, 120.15 g/mol) and poly(ethylene glycol) (PEO, 600 g/mol). DEG was the lower molecular mass *organic* model compound used. PEO, having a much lower molecular mass than Pluronic was the *polymeric* model compound, considered as the *bridging compound* between lower molecular mass DEG and higher molecular mass Pluronic.

The work included the synthesis of sulphonic acid and quaternary ammonium bromide derivatives of the Pluronic carriers. However, in this study, only the amine-terminated Pluronic (amino-pluronic) was considered for use to test the affinity separation hypothesis. This was to:

- test the feasibility of such synthesis reactions;
- establish synthesis routes; and

- lay down foundation for further study on ionic affinity separation.

Cibacron Blue 3GA has an affinity for serum albumin and this selectivity association was used as model to test the affinity separation hypothesis. In the protocol followed, Cibacron Blue 3GA was coupled to the amino-pluronic carrier to form the ligand-carrier CBAP [Cibacron Blue 3GA-(amino-pluronic)]. Because Pluronic adsorbs onto polysulphone and can be remove by rinsing with Triton X-100, the CBAP ligand-carrier could provide a reversible albumin-binding site.

The preparation of the CBAP carrier was followed by its immobilisation onto an inert hydrophobic polymer substrate matrix. A dense-skinned narrow bore polysulphone membrane (membrane contactor) was selected and used as the inert hydrophobic polymer substrate matrix. For the purpose of this study, only the membrane material's hydrophobicity/adsorption property was considered, and not the transport properties of the capillary membrane.

The effectiveness of CBAP to isolate serum albumin was tested first on a single-fibre polysulphone matrix (the single-fibre CBAP-PSf) and later on a multi-fibre polysulphone matrix (the multi-fibre CBAP-PSf). The effectiveness of the separation method was monitored by means of the Kaiser ninhydrin test for the *qualitative* detection of proteins, and the Pierce™ protein assay for the *quantitative* detection of proteins. Electro-spray mass spectroscopy (ESMS) and SDS-PAGE (Sodium dodecyl sulphate polyacrylamide gel electrophoresis) methods were later used for the specific characterisation of serum albumin in the eluate.

The study included the following tasks:

- determine the critical micelle concentration of Pluronic by measuring surface tension and adsorption properties of Pluronic onto a polysulphone membrane;
- spin dense-skinned capillary narrow bore polysulphone membranes to serve as the adsorption matrix for the affinity ligand carrier;
- prepare and characterize amino-pluronic (amine terminated Pluronic);
- prepare and characterize the pluronic-sulphonic acid (sulphonic acid terminated Pluronic);
- prepare pluronic-trimethylammonium bromide (quaternary ammonium bromide terminated Pluronic); and
- determine the efficiency of the CBAP-PSf system to isolate serum albumin from sheep serum.

The sequence of experiments to test the hypothesis was conducted as follows (Figure 12):

- convert the hydroxyl end-groups of Pluronic to primary amino groups;
- covalent attachment of Cibacron Blue 3GA onto amino-pluronic to form a Cibacron Blue 3GA amino-pluronic coupled molecule; and

- coat dense, narrow-bore polysulphone membranes with CBAP to form the CBAP-polysulphone affinity matrix.

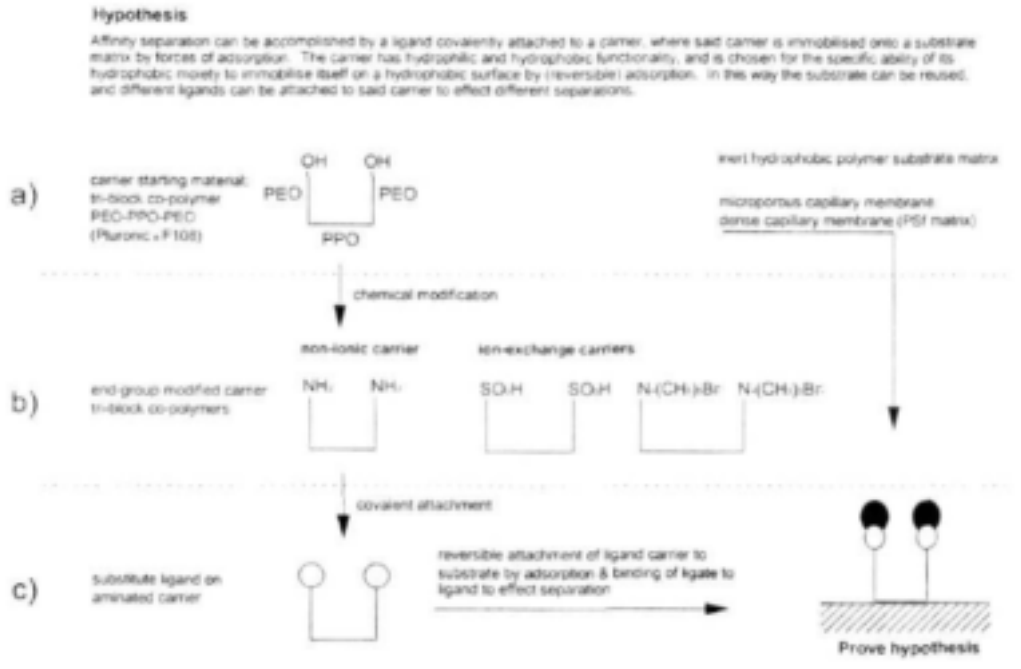

Figure 12: Hypothesis to test whether affinity separation can be effected by means of a ligand attached to a mobile ligand carrier, adsorbed onto a solid surface.

To isolate albumin from sheep serum, 5 ml serum, containing 5 mg/ml of protein was introduced into a multi-fibre cartridge. Buffer A (Table 4) was passed through the system for 6 h under constant UV-detection at 280 nm. Fractions were collected at 20-min intervals. Passing buffer B through the fibres for 4 h at said volumetric flow rate of 1.3 ml/min, eluted sheep serum proteins that were retained by the system. The fractions emerging from the system were collected at 25-min intervals, and the eluent was again monitored continuously at 280 nm.

Table 4: Composition of rinse and elution buffer solutions

Buffer A	0.05M Tris/HCl, pH 8.0, containing 0.05M NaCl
Buffer B	0.05M Tris/HCl, pH 8.0, containing 1M NaSCN

The protein concentration in the collected fractions was determined by the Pierce™ protein assay (Figure 13). After dialysis and freeze-drying the presence of sheep serum albumin in the collected fractions was established by ES-MS (not reported here) and SDS-PAGE (Figure 14).

Sheep serum was directly introduced into the multi-fibre column and buffer A was passed through the system to elute serum proteins which did not interact with the Cibacron Blue 3GA dye, until the buffer A fractions contained no serum proteins.

Buffer B was then introduced into the multi-fibre column to elute proteins retained on the fibres.

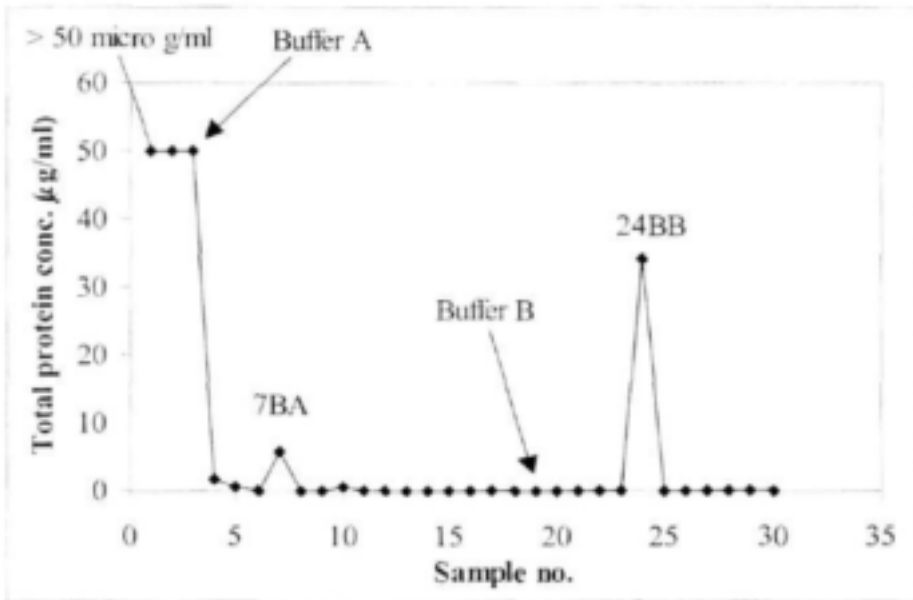

Figure 13: Concentration of sheep serum proteins (µg/ml) in the various fractions (sample no.) after affinity separation on a CBAP-PSf matrix, using buffers A and B.

Fractions 7BA (a buffer A fraction) and 24BB (a buffer B fraction) were analysed by ESMS and SDS-PAGE to detect possible presence of sheep serum. The results of ESMS and SDS-PAGE are shown in Figure 14.

The presence of sheep serum albumin in fractions 7BA and 24BB was confirmed by SDS-PAGE. Both samples showed bands that co migrated with BSA (Figure 14). In fraction 7BA (lane 8), however, several additional bands could be seen indicating that the fraction was not pure serum albumin. Fraction 24BB (lane 9) eluted from the CBAP-PSf affinity matrix in buffer B, showed only a single band corresponding to the BSA in lanes 6 and 7. It is apparent from the results that sheep serum albumin could indeed be separated effectively from the other serum proteins using the CBAP-PSf affinity matrix, and later eluted with a specific elution buffer. The degree of purification is seen when the content of lanes 1 to 4 is compared with lane 9.

3.5 Conclusions

Although other experiments provided support of the theory, the study on the isolation of sheep serum albumin from sheep serum provided the final proof that the hypothesis of an adsorptive-carrier, mediating affinity separation, cannot be rejected.

Cibacron Blue 3GA, covalently coupled to the carrier amino-pluronic coated polysulphone matrix, effectively separates albumin from serum. The preliminary

isolation of sheep serum albumin from sheep serum was first carried out on a single fibre CBAP-PSf matrix, to test the efficiency of the method, and concluded on a multi-fibre CBAP-PSf matrix. The results obtained with the multi-fibre system indicated that the technique could be used in preparative separations.

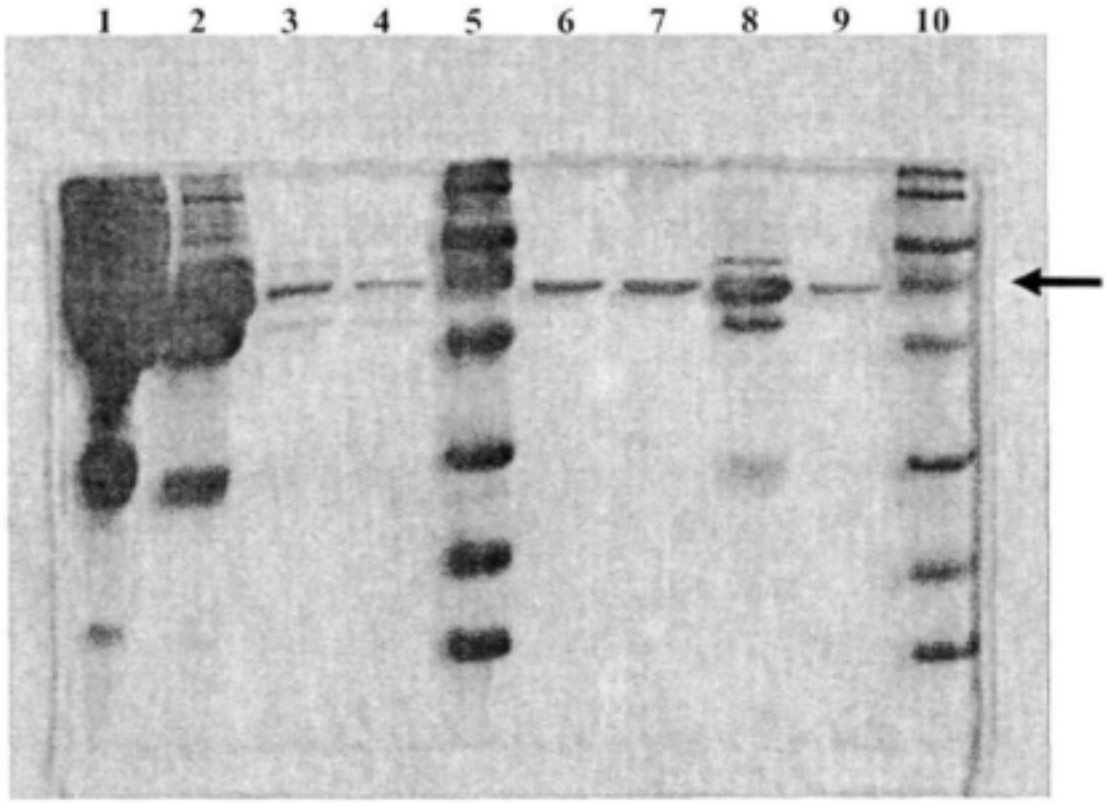

Figure 14: SDS-polyacrylamide gel analysis of sheep serum, commercial BSA and fractions 7BA and 24BB. Lanes (1), (2), (3) and (4): diluted sheep serum samples (×2, ×10, ×50, ×200 respectively); (5) and (10): low-molecular-mass protein standards; (6) and (7): commercial BSA; (8): fraction 7BA; (9): fraction 24BB. (The arrow indicates a molecular mass of 66 000 Daltons (BSA).

4.0 Axial flow module and manifold development

4.1 Introduction

Various transverse-flow membrane reactors were developed at the beginning of this programme. The technology was made available to another WRC research programme (K5/931) for further development, characterisation and application. That information is available in a final WRC report.

The focus on module development gravitated to the development of more effective and inexpensive axial flow modules. Various lines of thought were followed and evaluated concerning alternative designs for the module (scale-up of filtration area, materials of construction, cost, etc) and the manifolding system. All of these are discussed in the paragraphs to follow.

4.2 Manifold development

The 90^{ϕ} mm cartridges were manufactured (Figure 15) to slide-fit into the side-branches of standard 110 mm u-PVC T-pieces. The manifold consists of individual T-pieces that are either flanged (Figure 16) or solvent-welded (Figure 17a) together to form the manifold. The modules are provided with two O-rings, which create the hydraulic seal between the 110 mm tube-sheet on the module and the side-branch of the u-PVC T-piece. The downside of this simple technique to create a filtration loop was that the top and bottom manifolds needed to be kept in place with cable stays to prevent them from telescoping under pressure.

Figure 15: 90 mm cartridge module that seals into the side-branch of a 110 mm T-piece by way of O-rings.

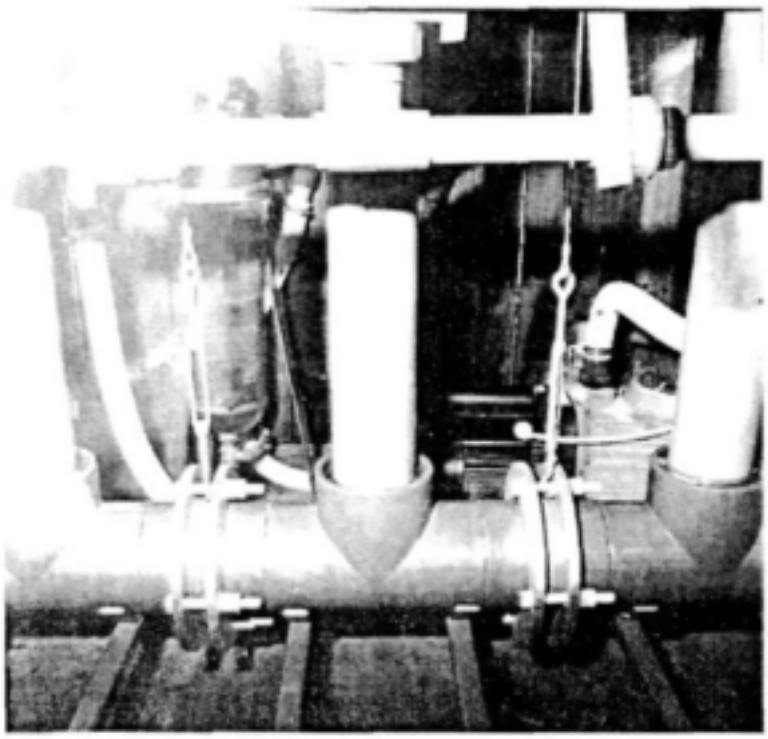

Figure 16: Flanged 110 mm T-pieces into which 90mm bayonet modules fits.

One of the problems experienced with the above module design (Figure 15) is that the O-ring seals tend to freeze into place after months of operation. Removal of one module from a rack is therefore not always a trivial task, because the manifolds needed to be dismantled. (The manifold design shown in Figure 16 simplifies the removal of a single module, since unbolting the flange coupling between T-pieces allows access to individual modules. The increase in cost is a deterrent though). Various other ways to construct the manifold was considered and evaluated in the laboratory and in the field. At that point in time all efforts were directed to reduce the cost of the membrane/manifold system and increase the module packing density in a manifold arrangement.

Principally one can adopt a number of approaches to construct a manifold arrangement to accommodate up to eight of the bayonet-type 90 mm modules (Figure 17b, Figure 17c). In one example, use is made of three solvent welded 90mm T-pieces to make up a three-module manifold section, and these are bolted together so that only three modules needed to be removed to access a particular module. In this case the side-branches are fitted with 110x90 mm reducing bushes that were first machined to provide O-ring grooves before the reducing bushes were solvent-welded onto the side-branch. A 110 mm plain socket was machined to slide-fit over the module tube-sheet and manifold side-branch extension. The 110 mm socket may be moved either down or upwards over the O-rings to facilitate and simplify the removal of individual modules from a rack, without having to remove the manifold. The idea works very well in practice, but the 35% reduction in overall cost for such a set of manifolds have to be weighed up against savings in effort to part dismantle the manifold section to remove modules if the O-rings became stuck. These 90 mm

manifold systems also have to be supported within an external structure, or restrained from telescoping with stainless steel tension cables. However, the overall height of the module installation is greater than that of the standard 110 mm T-pieces shown in Figure 17a.

An even less expensive way to accommodate the 90 mm modules in a similar way as the above is to melt-weld 90mm side branches to 110 mm pipe sections and provide those with an O-ring collar (Figure 17c). The advantage is that the lateral spacing of the modules is now not a function of the size of the T-piece section any more.

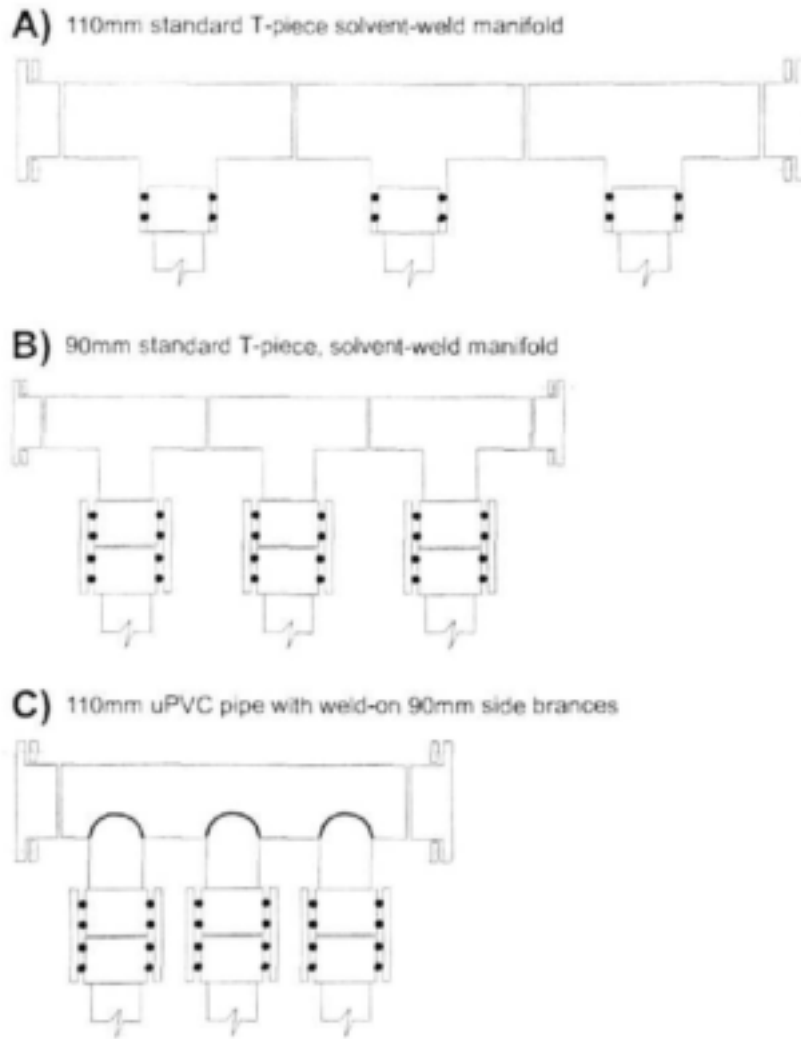

Figure 17: Different manifold designs for a 90mm module.

Alternative methods to provide a hydraulic seal between the module tube-sheet and the manifold were also investigated. If the tube-sheets are moulded correctly, the use of a second O-ring is superfluous. The use of lip seals will also ensure drip-free operation, with the advantage of a 5% increase in membrane area and 6% reduction in tube-sheet moulding compound. There is little difference between the cost of a lip

seal and that of two O-rings. One could fabricate O-rings from O-ring cord, but the disadvantage is that such O-rings do break from time to time when the modules are disturbed, causing leaks.

A substantial saving in cost can be brought about if more than one module is connected in series between the inlet and outlet manifolds (Figure 18). If three modules are for example connected between the inlet and outlet manifolds, the cost of two manifold sets can be saved for the price of two plain sockets. Sliding the 110 mm socket over the O-rings seals the middle section of the module arrangement. This approach was tested successfully in the laboratory and can be applied in situations of both dead-end and cross-flow filtration. In some way this emulates the X-Flow BV filtration approach, whereby cartridges are placed in series within a pressure vessel, very much in the way that spiral wrap elements are accommodated within a pressure vessel.

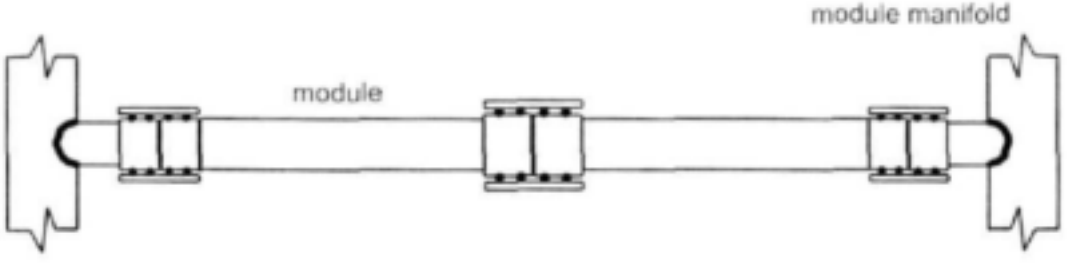

Figure 18: In-line module connection configuration, manifolded at the far ends of the module train.

4.3 Module development

The development of larger sized axial-flow modules received attention during the latter part of the project. Both the arrangements investigated have membrane filtration areas in excess of 20 m^2. The principle difference between the two is that the design criteria of one version will be based on modelling studies of the pressure distribution and flow patterns in such a module. This will be discussed in later paragraphs. The product of this module will be drawn from the shell side.

The second version operates on a different principle. Here the membrane cartridge will be placed inside a pressure vessel, and the product taken from a collecting tube in the centre of the module.

4.3.1 Central product withdrawal module

Figure 6 shows a schematic diagram of the in-line module developed by X-Flow. This approach allows the modules to be positioned horizontally, which decreases the footprint of an installation. However, great care has to be exercised during the construction of this module type. These modules, as is the case with flat-sheet spiral wrap designs, are prone to O-ring failure and the product being contaminated by feed water. With the 90 mm cartridge design, the product can only be contaminated when

fibres break. The in-line module under discussion here, other than the configuration disclosed in Figure 18, can be prone to leakage caused by poor quality control during fabrication and poor bonding between the tube-sheet moulding compound and the shroud. Although it is not difficult to engineer leak-free adhesion between the tube-sheet plug and the u-PVC shell with proper choice of materials, the possibility of leaks past O-ring seals remains of general concern.

The lip-seal is dependent on the head-loss across the length of the module to force the lip-seal against the inside of the pressure vessel, thereby providing a necessary tight seal to channel the process water across the membrane lumen.

The in-line design is more costly than that of the cartridge/bayonet design, both in materials of construction and labour. Manifolding is simpler, but removal of modules to repair compromised fibres is more difficult. The in-line module arrangement shown in Figure 18 would be a less expensive way to accommodate modules in that configuration as opposed to that shown in Figure 19, where a pressure vessels is required to house the membrane cartridge. So, if required, the approach shown in Figure 18 would be adopted if membranes were required to be installed in-line.

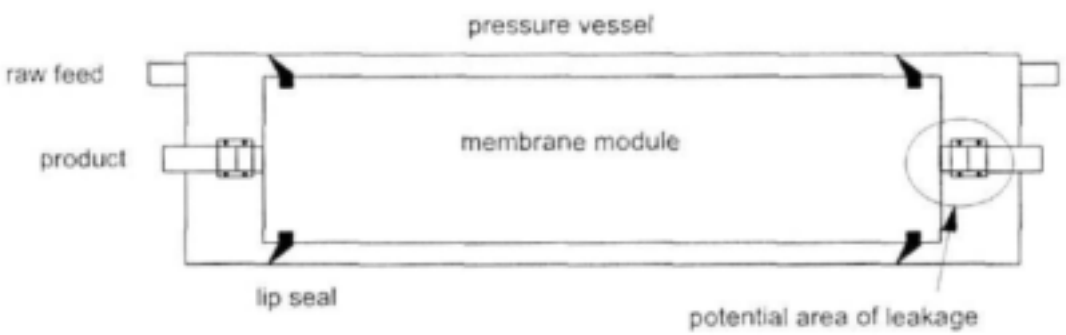

Figure 19: In-line membrane element arrangement, module housed inside pressure vessel.

After much experimentation, cost comparison and ease of operability, the final choice for module manifolding resorted to flanges. Two module sizes were experimented with. In the one case the module shroud was constructed from 110 mm u-PVC and the modules house 7 m^2 membrane filtration area (Figure 16). In the second design the shroud is constructed from rolled stainless steel plate, and the module houses 25 m^2 membrane filtration area. To accommodate the modules the manifold can be constructed either as per the examples shown in Figure 17b or Figure 17c, but with a flange stub instead of the O-ring containing spigot.

With the flanged-type modules, the tube-sheet potting material not only encases the membranes and seals the shroud, but the material also has to be of great enough strength to accommodate the tensile forces in act during operation. In earlier manifold designs cable stays prevented the manifolds from pulling apart under pressures that can be as high as 3 bar. V-band clamps and the mechanical integrity of the flange casting provide that function in the designs shown in Figure 21.

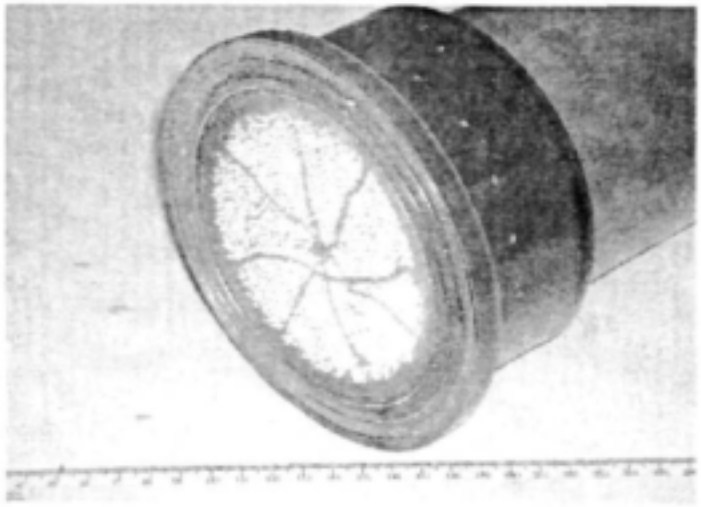

Figure 20: Flanged 110mm capillary membrane module containing 7m^2 filtration area.

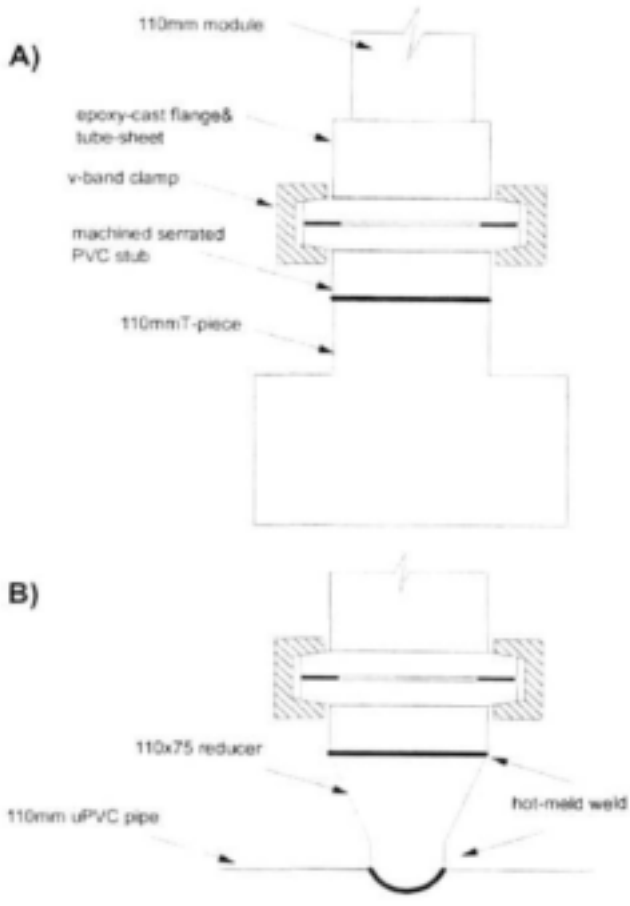

Figure 21: Modules fitted with flanges and secured to the manifold by means of V-band clamps.

Choice of potting material was particularly troublesome during the development of the flanged tube-sheet of the 200 mm module. The casting material that was developed to encase membranes in the bayonet-type modules during a previous WRC research project shrunk slightly during curing and post-curing. Although this was of little concern during the fabrication of 90 mm bayonet-type modules, shrinking became a major obstacle to progress during the development of especially the 200 mm modules because it lead to the formation of stress fractures in the tube-sheet.

There are a number of criteria that a potting compound has to fulfil to be useful as a tube-sheet casting compound and in larger-sized modules, shrinking is an important one. Potting compounds with the required properties were not available off the shelf. A potting compound had therefore to be constituted through experimentation, which delayed the development of the 200 mm module by nearly 6 months. None-the-less, the final product that were developed passed the test in that the flanged module shown in Figure 22 was pressure-tested at pressures up to 10 bar for weeks without any problem.

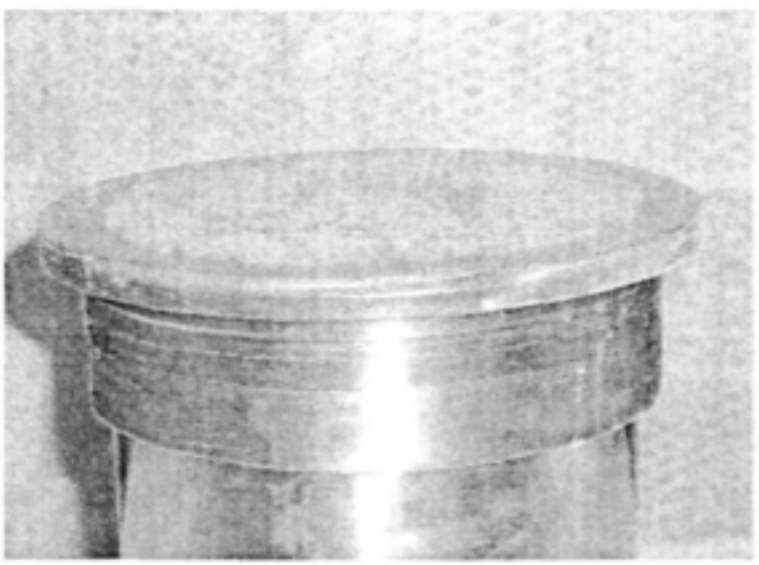

Figure 22: Stainless steel shrouded 200 mm axial-flow module containing 23 m^2 membrane filtration area.

4.4 Computational fluid dynamic modelling

The aim of this work is to develop an effective axial-flow module concerning geometry. It includes the modelling of the flow behaviour inside such a module, i.e. the pressure and velocity profiles which exist in the lumen and shell sides. The lumen refers to the inside of the capillaries while the shell refers to the outside region surrounding the capillaries.

Several contributions have been made toward modelling the hydrodynamics in hollow-fibre systems. Most of these models are based on the assumption that the flow associated with each fibre is identical, so that a single fibre with its surrounding fluid

annulus is representative of the whole fibre bundle. Krogh[16] made the first contribution when he made calculations on the oxygen pressure head required in capillaries in muscles. He assumed that all the capillaries have the same multi-fibre geometry. In his honour, the single representative fibre unit is called the Krogh cylinder. The Krogh cylinder has an outer radius, R_S, which is the radius of the surrounding fluid annulus. It is defined such that the porosity of a single fibre unit is the same as the porosity of the whole fibre bundle. Also, the fibres are assumed to be arranged in a regular array with no fluid exchange between adjacent Krogh cylinders. Radial pressure gradients are also neglected.

The Krogh cylinder model (KCM) was used as the basis for modelling by several authors [e.g. Apelblat *et al.*,[17] Bruining, [18] Kelsey *et al.*[19] and Pangrle *et al.*[20]]. They all used different combinations of the Navier-Stokes equation and Darcy's Law. However, their primary weakness is the lack of incorporation of the interfibre flows in the shell side, as well as the macroscopic radial pressure gradients. Since the hydrophilic fibres expand when wetted, they assume a wavy appearance, because they are cast within tube-sheets at both ends of the module. Hence the Krogh cylinder approach fails and different modelling techniques are required.

Labecki *et al.*[21] proposed a new model, the porous medium model (PMM), which encompasses all fibres and has a spatial domain corresponding to the actual dimensions of the entire module. Using this new approach, the lumen and shell are treated as two interpenetrating porous regions with a continually, spatially dependent source/sink of incompressible fluid. The steady-state continuity equation is then applied to both the lumen and the shell, yielding

$$\nabla \cdot \underline{V}_S = \phi \qquad \textbf{Equation 1}$$

and

$$\nabla \cdot \underline{V}_L = -\phi \qquad \textbf{Equation 2}$$

---

[16] Krogh, A., 1919, The number and distribution of capillaries in muscles with calculations of the oxygen pressure head necessary for supplying the tissue. *J. Physiol.* **52**, 409-415.

[17] Apelblat, A., Katzir-Katchalsky, A. and Silberberg, A., 1974, A mathematical analysis of capillary-tissue exchange. *Biorheology* **11**, 1-49.

[18] Bruining, W.J., 1989, A general description of flows and pressures in hollow fiber membrane modules. *Chem. Engng. Sci.* **44**, 1441-1447.

[19] Kelsey, L.J., Pillarella, M.R. and Zydney, A.L., 1990, Theoretical analysis of convective flow profiles in a hollow-fiber membrane bioreactor. *Chem. Engng. Sci.* **45**, 3211-3220.

[20] Pangrle, B.J., Alexandrou, A.N., Dixon, A.G. and DiBiasio, D., 1991, An analysis of laminar fluid flow in porous tube and shell systems. *Chem. Engng. Sci.* **46**, 2847-2855.

[21] Labecki, M., Piret, J.M. and Bowen, B.D., 1995, Two-dimensional analysis of fluid flow in hollow-fibre modules. *Chem. Engng. Sci.* **50**, 3369-3384.

where $\underline{V}_S$ and $\underline{V}_L$ are the shell and lumen superficial velocity vectors and ϕ is the fluid source/sink term:

$$\phi = \frac{L_p A_v}{\mu}(P_L - P_S) \qquad \textbf{Equation 3}$$

Darcy's Law for the shell and lumen is given by

$$\underline{V}_S = -\frac{1}{\mu}\left(\underline{1}_x k_{x,S}\frac{\partial P_S}{\partial x} + \underline{1}_r k_{r,S}\frac{\partial P_S}{\partial r}\right) \qquad \textbf{Equation 4}$$

and

$$\underline{V}_L = -\frac{1}{\mu}\left(\underline{1}_x k_{x,L}\frac{\partial P_L}{\partial x} + \underline{1}_r k_{r,L}\frac{\partial P_L}{\partial r}\right) \qquad \textbf{Equation 5}$$

However, the fibres are not directly connected to each other, so the average lumen flow is one-dimensional and $k_{r,L}$ can be set to zero. Thus Equation 5 becomes

$$\underline{V}_L = -\frac{1}{\mu}\left(\underline{1}_x k_{x,L}\frac{\partial P_L}{\partial x}\right) \qquad \textbf{Equation 6}$$

Equation 1 is combined with Equation 4 and Equation 2 with Equation 6, yielding the following pair of coupled partial differential equations for $P_L(x,r)$ and $P_S(x,r)$ respectively:

$$-k_{r,S}\frac{1}{r}\frac{\partial}{\partial r}\left(r\frac{\partial P_S}{\partial r}\right) - k_{x,S}\frac{\partial^2 P_S}{\partial x^2} = L_p A_v (P_L - P_S) \qquad \textbf{Equation 7}$$

$$k_{x,L}\frac{\partial^2 P_L}{\partial x^2} = L_p A_v (P_L - P_S) \qquad \textbf{Equation 8}$$

These two equations cannot be solved analytically and numerical methods have to be employed. In this study, a finite element software package, Fastflo, was used. It was specifically written for the numerical solution of partial differential equations (PDEs) in two and three dimensions and eliminates the need for time-consuming programming in languages such as FORTRAN.

The flux, as predicted by Fastflo, is calculated as follows. After solving for Equations 7 and 8, the normal component of Equation 5 is numerically integrated over the inlet and outlet flow areas to obtain the lumen inlet and outlet flow rates. The difference, by subtraction, is the shell outlet or permeate flow rate. The flux is obtained by dividing the permeate flow rate by the total effective membrane area in the module.

4.4.1 Model parameters

Several parameters must be specified in Fastflo's problem file. One of these, the outlet lumen pressure, $P_{L,out}$, depends on the axial pressure drop, ΔP, along the module. The axial pressure drop is calculated by making use of Kelsey's 1-D model and the Hagen-Poiseuille equation[22].

Hagen-Poiseuille: $\Delta P = \frac{8\mu L}{\pi r_L^4} \cdot \frac{Q_{feed}}{N}$, where $Q_{feed} = uA_{flow}$ **Equation 9**

Kelsey's 1-D model: $Q_{feed} = \alpha(\lambda B_1 + B_3)$ **Equation 10**

where

$$\alpha = -\frac{N\pi r_L^4}{8\mu L_{wet}}$$ **Equation 11**

$$\lambda = 4\sqrt{\kappa(1+1/\gamma)}$$ **Equation 12**

$$\kappa = \frac{L_p L_{wet}^2}{r_L^3}$$ **Equation 13**

$$\gamma = \left(\frac{1}{r_L^4}\right)\left[4r_S^4 \ln(r_S/r_M) + 4r_S^2 r_M^2 - 3r_S^4 - r_M^4\right]$$ **Equation 14**

$$B_1 = \frac{(P_{S,out} - P_{L,in})[\cosh(\lambda)-1] + (P_{L,out} - P_{L,in})\left[1+\frac{\cosh(\lambda)}{\gamma}\right]}{\left[\frac{\lambda}{\gamma} - \sinh(\lambda)\right][\cosh(\lambda)-1] + \left[\frac{\lambda}{\gamma} + \sinh(\lambda)\right]\left[1+\frac{\cosh(\lambda)}{\gamma}\right]}$$ **Equation 15**

$$B_3 = \frac{\lambda}{\gamma} B_1$$ **Equation 16**

In this study, the inlet flow velocity, u, is specified as 1.2 m/s. Instead of guessing a value for ΔP in order to obtain a value for $P_{S,out}$ in Equation 15, ΔP is estimated by using the H-P equation. Kelsey's 1-D model is then used to predict the lumen feed

---

[22] Yoshikawa, S., Ogawa, K., Minegishi, S., Eguchi, T., Nakatani, Y. and Tani, N., 1992, Experimental study of flow mechanics in a hollow-fiber membrane module for plasma separation. *J. Chem. Eng. Japan* **25**, 515-521.

flow rate, from which the inlet flow velocity is calculated. If this is not equal to 1.2 m/s, ΔP and thus the outlet lumen pressure are adjusted iteratively until the inlet flow velocity is equal to 1.2 m/s. The value for ΔP, which yields an inlet flow velocity of 1.2 m/s, is then used in Fastflo. This procedure was repeated for all the various module lengths.

The membrane permeability, L_p, must also be determined beforehand. The permeability of the membranes was determined using the PMM and is calculated by

$$L_p = \frac{\mu Q}{A \Delta p_m} \qquad \textbf{Equation 17}$$

where Q is the experimental transmembrane flow rate, or permeation flow rate, A is the total membrane surface area and Δp_m is the transmembrane pressure drop. In the cross-flow filtration mode, the transmembrane pressure drop is difficult to determine. The pressure drop, Δp, between the lumen inlet and shell outlet in the dead-end filtation mode, is more easily measured, since the entire pressure drop occurs across the membrane. This approximation is used to determine the apparent permeability:

$$L_{p,app} = \frac{\mu Q}{A \Delta p} \qquad \textbf{Equation 18}$$

The procedure is as follows: using the dead-end mode, the lumen inlet pressure is set to a known, fixed value, while the shell outlet pressure is kept at 0 kPa. Thus Δp is specified. With μ and A also specified, the actual L_p is treated as a variable input parameter. The flow rate, Q, is then calculated with the PMM by numerically integrating the normal component of the superficial velocity over either the inlet or outlet flow area. This value of Q is then used to calculate the apparent permeability, $L_{p,app}$. Finally, a correction plot of $L_{p,app}$ vs. L_p is obtained. Q and Δp is then measured experimentally in the dead-end mode and $L_{p,app}$ is calculated from Equation 18. The correction plot is used to obtain the true permeability.

Five different dead-end module configurations were used. These are:

- A – downstream permeate outlet open;
- B – upstream permeate outlet open;
- C – downstream and upstream permeate outlets open;
- D – downstream and upstream permeate outlets open (feed entrance from both sides); and
- E – permeate outlet halfway down the module length.

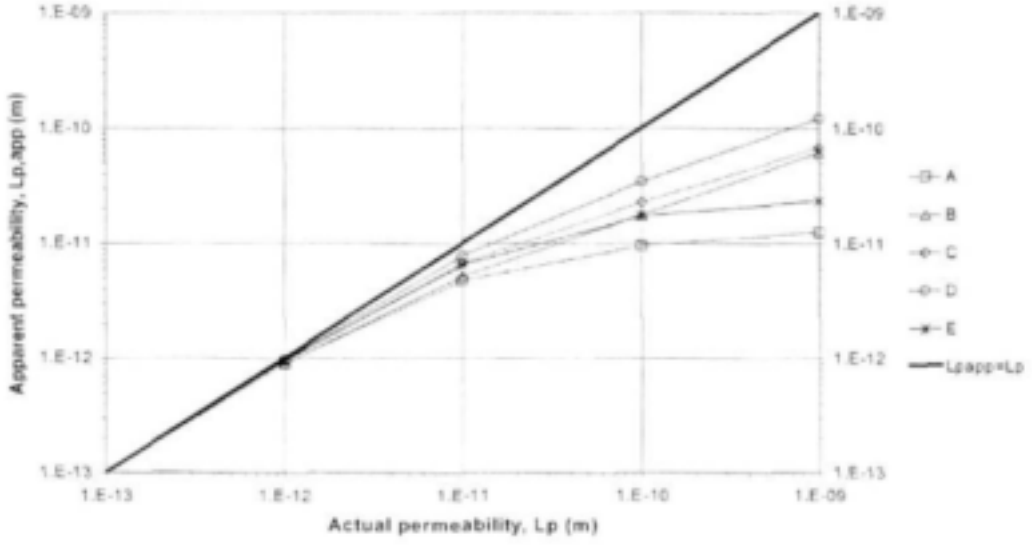

Figure 23: Correction plot for membrane permeability.

Using a 50 mm diameter module with a length of 1.2 m, configuration D seemed to deviate the least from the $L_p = L_{p,app}$ line, thus producing the best estimate for the membrane permeability. An experimental flow rate of 114 L/h was measured, yielding an apparent permeability of 2.3E-13 m. This corresponds to an actual permeability of 2.3E-13 m, according to the correction plot.

Fastflo was used to predict the flux for modules of various lengths and outside diameters in the cross-flow filtration mode. The permeate outlet was set in 3 positions, namely upstream, downstream and halfway down the length of each module. A packing density of 62.2% was used in each module. The diameters and corresponding number of membranes used are given in Table 5. The membrane lengths and corresponding pressure drops are given in Table 6.

Table 5: Shroud outside and inside diameter and number of capillaries per shroud

OD/ID (mm)	20/17	25/22	32/29	40/37	50/42	63/55
N	55	93	161	263	339	581
OD/ID (mm)	75/65	90/80	110/100	125/115	140/130	160/150
N	812	1229	1921	2540	3246	4321
OD/ID (mm)	200/190	250/240.2	315/302.6	355/341	400/384.4	
N	6933	11079	17584	22330	28375	

Table 6: Capillary membrane length and corresponding head-loss

L (m)	0.5	0.6	0.7	0.8	0.9	1.0	1.1	1.2
ΔP (Pa)	10 729	13 510	16 275	19 025	21 758	24 478	27 185	29 880

Since the PMM also considers wet capillary membrane expansion, it was found that on average the length of the membranes increased by 7% when wetted. Other parameters used are given in Table 7. All pressures are gauge pressures.

Table 7: Other parameters used in model

r_L (mm)	r_M (mm)	μ (Pa.s)	L_p (m)	$P_{L,in}$ (Pa)	$P_{S,out}$ (Pa)
1.2	1.8	0.001002	2.3E-13	100 000	0

It was found that the highest flux values were obtained with the permeate outlet positioned halfway down the length of the module, as shown in an example below. A permeate outlet located in the upstream position produced the lowest flux values.

The flux values (Lmh) obtained with the permeate outlet located halfway down the length of each module are tabulated in Table 8.

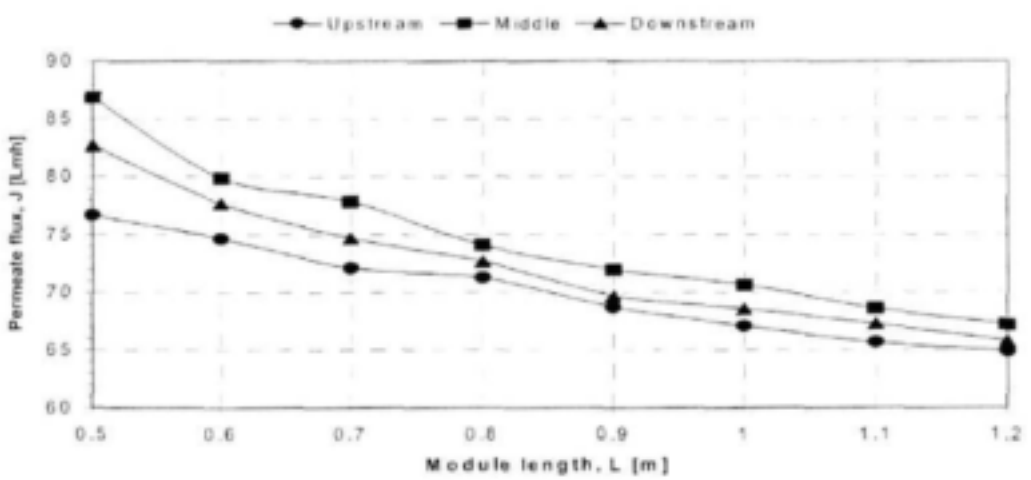

Figure 24: Flux prediction as a function of module length and position of permeate outlet.

4.5 COST CALCULATIONS

Although the flux for various module geometries was predicted, we need to know which module diameter would be the most economical. We can do this by expressing the costs of each module in terms of a cost per unit volume permeate produced. The cost of each module comprised two components. The *capital cost* includes the cost of the module outer shell and the membranes, while the *operating cost* is the cost of pumping energy. The cost of pumps, piping and pipe fittings are excluded for simplification.

Table 8: Flux values of different modules with permeate outlet in middle

D ↓	L →	0.5m	0.6m	0.7m	0.8m	0.9m	1.0m	1.1m	1.2m
20mm		71.91	64.38	61.99	60.12	58.52	57.29	55.82	54.60
25mm		75.26	69.05	65.83	64.35	62.32	60.42	59.12	57.81
32mm		78.89	72.56	69.26	67.44	65.29	63.79	62.19	60.66
40mm		81.86	74.40	71.84	69.31	67.40	65.67	64.13	62.83
50mm		81.82	75.20	71.67	70.29	68.62	66.74	65.27	63.86
63mm		84.01	77.33	74.82	72.05	70.24	68.21	66.81	65.54
75mm		84.94	77.84	76.07	73.19	71.18	69.41	68.00	66.32
90mm		86.81	79.84	77.82	74.09	71.94	70.62	68.61	67.18
110mm		87.65	81.69	77.74	75.02	72.59	71.31	69.60	68.00
125mm		88.84	81.75	78.13	75.48	73.35	71.52	69.85	68.44
140mm		88.69	83.37	78.71	75.70	73.64	71.94	70.25	68.80
160mm		89.44	83.24	79.27	75.92	74.15	72.10	70.69	69.28
200mm		91.41	83.26	79.73	76.42	74.47	72.81	71.10	69.68
250mm		90.61	84.29	79.52	76.93	74.72	72.88	71.33	69.89
315mm		91.94	84.09	79.42	77.50	75.26	73.35	71.87	70.17
355mm		91.12	84.65	79.26	77.38	75.49	73.75	71.90	70.25
400mm		92.89	85.08	79.71	77.61	75.31	73.79	71.92	70.37

4.5.1 Time value of money and discount factors

When performing cost calculations, we often encounter the problem of having to combine capital and operating costs. Capital costs are fixed and are measured in Rands, whereas operating costs are measured in Rands per unit time, typically Rands per year. These two costs must be placed on the same basis and we do this by making use of the time value of money (TVM). The easiest method is to annualise the capital costs and report all costs on an annual basis. The TVM is determined by expressing a single capital expenditure/investment as a series of equal payments (PMT), or annuities, spread over a certain number of years. These annual payments have the same units as operating costs. Douglas[23] uses a discount factor, the capital charge factor (CCF), to account for the TVM. The present value (PV) of the capital investment is multiplied by the CCF to obtain an annuity. The CCF is given by:

$$CCF = \frac{[0.25(1+i)^4 + 0.295i - 0.298](1+i)^N - 0.225i + 0.048}{0.676[(1+i)^N - 1]} \qquad \textbf{Equation 19}$$

where i is the interest rate per year and N the lifespan of the membrane plant in years.

[23] Douglas, J.M. (1988). Conceptual design of chemical processes. Singapore: McGraw-Hill, Inc.

Assuming the interest rate to be 15% per year and an operating life of the membrane plant of 5 years, this yields a CCF of 0.57. However, CCF is intended for performing cost calculations of large chemical plants as it includes revenue, working capital, start-up costs and total production costs.

A membrane filtration plant is much smaller and simpler in comparison and the capital recovery factor, CRF[24], would be a more suitable discount factor. The PV of an annuity is given by[25]:

$$PV = PMT\left[\frac{1}{i} - \frac{1}{i(1+i)^N}\right] \qquad \textbf{Equation 20}$$

or

$$PV = PMT\left[\frac{(1+i)^N - 1}{i(1+i)^N}\right] \qquad \textbf{Equation 21}$$

Capital cost is thus annualised by multiplying the PV by the CRF:

$$\text{PMT (R/yr)} = \text{PV (R)} \times \text{CRF (1/yr)} \qquad \textbf{Equation 22}$$

where

$$CRF = \left[\frac{i(1+i)^N}{(1+i)^N - 1}\right] \qquad \textbf{Equation 23}$$

Using an interest rate of 15% and a plant life of 5 years, this gives a CRF = 0.3. This value will be used to annualise capital costs in this study.

4.5.2 Cost comparisons

In order to find the most cost effective module in terms of cost per unit volume permeate produced, a spreadsheet was developed by Marais[26]. The optimum module geometry, and thus cost, will depend on the product flow rate required. For the purpose of this study, it was assumed that the required product flow rate is 1 000 L/h. Capital cost consists of the cost of fibres and module housing, while operating cost is

---

[24] Turton, R.B., Bailie, R.C., Whiting, W.B., & Shaeiwitz. (1998). Analysis, synthesis and design of chemical processes. Upper Saddle River, New Jersey: Prentice Hall.

[25] Brigham, E.F., & Houston, J.F. (1998). Fundamentals of Financial Management (8th ed.). Fort Worth, Texas: The Dryden Press.

[26] Marais, C. (2001).The hydrodynamic characterisation of an axial-flow membrane module. Masters thesis, University of Stellenbosch.

determined by the pumping energy. Details of all costs involved are provided elsewhere[26]. The following assumptions were also made:

- inlet flow rate 1.2 m/s
- inlet lumen pressure 100 kPa
- operating time 8 000 h/year
- pump efficiency 70%
- cost of electricity 30.27c/kWh

For each combination of module length and outer diameter, the cost per kL permeate produced was calculated by first determining the membrane area required to produce the desired product flow rate:

$$A_{req} = \frac{\text{Required product flow rate}}{Flux} = \frac{Q_{req}}{J} \qquad \textbf{Equation 24}$$

From this, the number of modules (rounded up to the nearest integer) that must be used, can be determined:

$$N = \frac{\text{Required membrane area}}{\text{Membrane area per module}} = \frac{A_{req}}{A_m} \qquad \textbf{Equation 25}$$

The actual membrane area used will always be more than that required, although the ratio between the two will in some cases be close to unity. The actual membrane area is given by:

$$A_{tot} = N \times A_m \qquad \textbf{Equation 26}$$

Similarly, the actual *permeate* flow rate that can be produced, will be more than that required:

$$Q_{act} = J \times A_{tot} \qquad \textbf{Equation 27}$$

The total *feed* flow rate to the system depends on the number of modules to be used:

$$Q_{feed} = u \times A_{flow} \times N \qquad \textbf{Equation 28}$$

The energy consumption can now be calculated:

$$E = C\frac{\Delta P \times Q_{feed}}{\eta} \qquad \textbf{Equation 29}$$

The operating cost per year is calculated by considering the cost of electricity and the operating time per year :

$$C_{yr} = E \times C_{kWh} \times \theta$$ **Equation 30**

This can be expressed as a cost per kL permeate produced :

$$C_{pump} = \frac{C_{yr}}{\theta \times Q_{req}}$$ **Equation 31**

Last, the capital cost must be converted to the same basis as operating cost by making use of the capital recovery factor :

$$C_{cap} = \frac{C_{mod} \times N}{\theta \times Q_{act}}$$ **Equation 32**

Thus the total cost is the sum of operating cost and capital cost, expressed in cents per kL permeate. The results are graphically portrayed in Figure 26.

From Figure 26 one can see that modules with small diameters are very uneconomical, irrespective of their length. As the module diameter increases, cost decreases, but at a slowing rate. It appears that there is no benefit from using module diameters in excess of 160 mm, as all the cost curves remain relatively flat above this diameter. On the flipside of the coin, modules with a diameter less than 90 mm are too expensive. Another characteristic that is not easily observable in Figure 26, is the cost of modules with lengths of 0.5 m and 0.6 m, relative to other module lengths. This is shown more clearly in Figure 27, which shows the inverse relationship between cost and module length. The reason for the sudden reduction in cost for module lengths of 0.5 m and 0.6 m, stems from the membrane manufacturing approach adopted. The membranes are taken up on a reel with a circumference of 1.4 m. When the membranes are removed from the reel, they are automatically cut into lengths of ~1.4 m.

From this it is obvious that for the 0.5 m and 0.6 m lengths, two membrane unit lengths can be cut from a standard 1.4 m-long membrane, allowing a few extra cm at both ends for potting into the modules. For these two lengths, the wastage is minimal. Figure 28 shows how this is achieved. For any module length of 0.7 m and longer, only one membrane unit can be cut from the standard 1.4 m length. Much membrane is wasted for the 0.7 m length, but the wastage decreases with an increase in module length. This is summarized in Table 9.

Although the wastage of the two 0.6 m lengths and the one 1.2 m length is exactly the same, the overall cost depends on other factors, such as the cost of the module itself, as well.

From this discussion one can thus conclude that it would be best to use a module or series of modules having an outer diameter of between 90 mm and 160 mm and a length of 0.6 m.

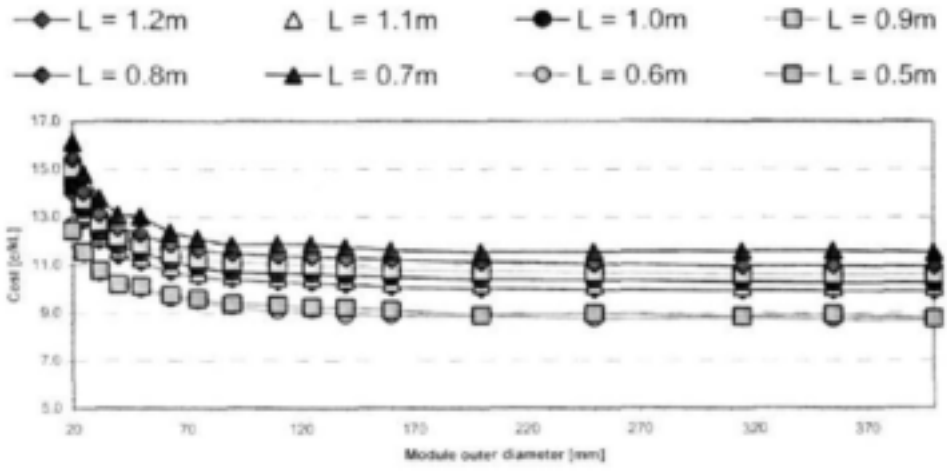

Figure 25: Actual cost chart for various module configurations for a required product flow rate of 1 000 L/h.

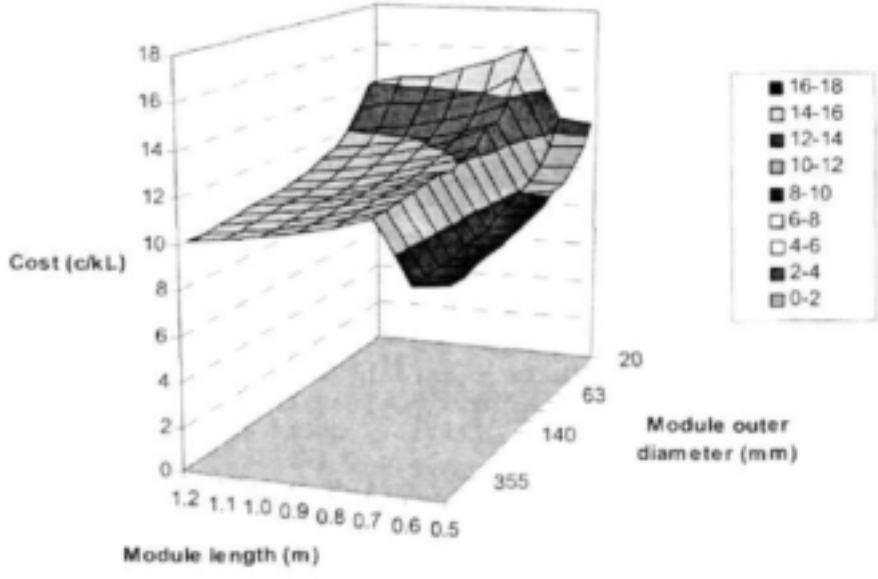

Figure 26: Surface chart for various module configurations for a required product flow rate of 1 000 L/h.

A stainless steel V-band clamp was developed to secure the 200 mm flanged module onto the manifold. It is relatively expensive to clamp the modules with stainless steel profile clamps, and a different option was implemented in the case of the 110 mm modules. A mould was subsequently developed to form sheet PVC into 120° profiles.

These profile sections are secured in place by means of T-bolt band clamps to provide a seal.

Table 9: Membrane wastage as a function of module length

Module length (m)	Wastage (m)	% wastage
2 × 0.5	0.4	28.6%
2 × 0.6	0.2	14.3%
1 × 0.7	0.7	50.0%
1 × 0.8	0.6	42.9%
1 × 0.9	0.5	35.7%
1 × 1.0	0.4	28.6%
1 × 1.1	0.3	21.4%
1 × 1.2	0.2	14.3%

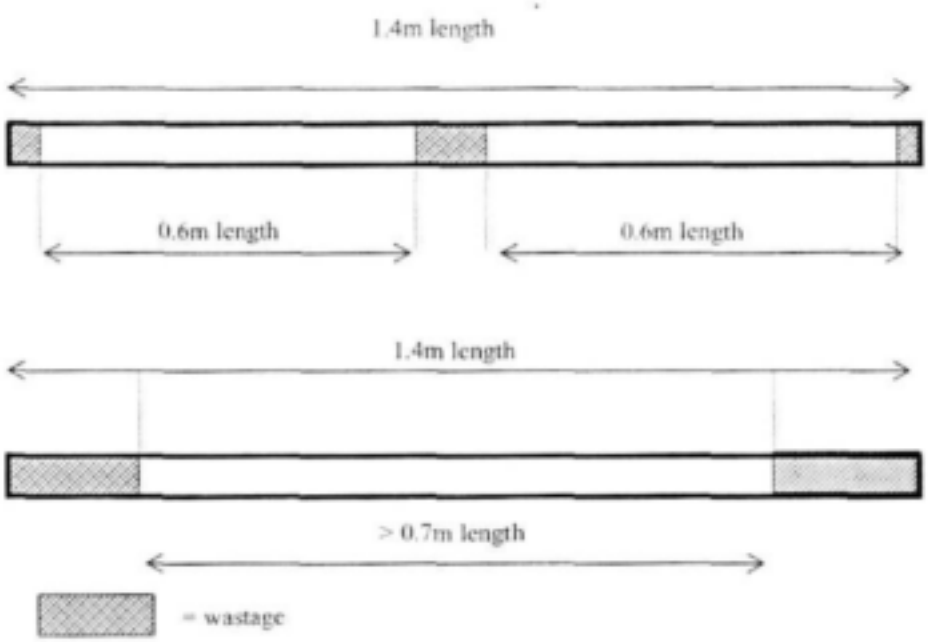

Figure 27: Membrane lengths and wastage.

4.6 Conclusions

From the stand of simplicity of fabrication, which is also a function of cost, a shell-and-tube axial flow module configuration was chosen as the standard design.

The computational fluid dynamics results indicated that there is some justification in choosing 110 mm and 200 mm shroud sizes as standard to house capillary membranes. These modules will respectively contain 7 and 25 m^2 membrane

filtration area. The eventual choice of shroud material was based on cost and reusability of the shroud material; 110 mm u-PVC and 200 mm welded stainless steel sheet.

In order to save on capital and operational cost for small membrane systems, it is anticipated that the ability to perform chemical cleaning *in situ* may not be engineered into small systems' design. For that reason it is essential that modules can be removed and replaced without much effort. Flanged-type coupling of modules to manifolds is therefore favoured, as opposed to the bayonet designs originally developed for the 90mm modules.

Various options are available to manifold the modules by means of flanges. A manifold consisting of T-pieces, solvent welded together, with a machined serrated stub hot-melt welded onto the side branch of a T-piece, is the preferred method to secure 110mm modules onto the manifold. In the case of the 200 mm module the same technique will not be used. It will be more cost effective to make use of a straight pipe section as the main manifold, onto which reducers are hot-melt welded. A machined 200 mm serrated stub will allow the module to be secured onto the flange by means of V-band clamps.

5.0 Conclusions

Membrane development

A new polysulphone membrane with a spongy substructure was successfully developed and tested in the field. This membrane had superior mechanical properties to that of the skinless membrane, which it superseded in potable water production applications. The membrane was extensively tested in the field.

A double-skinned poly(ether sulphone) membrane with a void-like substructure was also developed and evaluated in the field. No problems were incurred during field trials of the new membrane.

Mixing within spinneret flow passages can be improved by introducing shear planes to prevent spin-solution channelling within tube-in-tube spinnerets.

Membrane modification

Coating the membranes with Pluronic, a tri-block copolymer, non-ionic surfactant can alter the flux and cleaning properties of polysulphone membranes. No binding of proteins occurred if the membranes were coated with Pluronic. However, because of the low fluxes achieved with membranes coated with Pluronic, this approach to membrane performance enhancement was terminated.

As an alternative, the coating material was used as a mediator to effect other properties to a membrane. The suggestion to alter the Pluronic by covalent attachment of a ligand was researched in a successful study on the isolation of sheep serum albumin from sheep serum. This provided the necessary proof that the hypothesis of an adsorptive-carrier, mediating affinity separation, cannot be rejected.

Cibacron Blue 3GA (a ligand for albumin) was covalently coupled to Pluronic after the hydroxyl end-groups of the poly(ethylene oxide) side chains were first converted to primary amines. Polysulphone membranes were coated with the ligand-carrying Pluronic, yielding a polysulphone affinity matrix. The preliminary isolation of sheep serum albumin from sheep serum was first carried out on a single fibre CBAP-PSf matrix to test the efficiency of the method. The work was concluded on a multi-fibre CBAP-PSf matrix. The results obtained with the multi-fibre system indicated that the technique could be used in preparative separations.

Manifold and axial-flow capillary module development

From the stand of simplicity of fabrication, which is also a function of cost, a shell-and-tube axial flow module configuration was chosen as the standard design.

The computational fluid dynamics results indicated that there is some justification in choosing 110 mm and 200 mm shroud sizes as standard to house capillary membranes. These modules will respectively contain 7 and 25 m^2 filtration area. The eventual choice of shroud material was based on cost and reusability of the shroud material; 110 mm u-PVC and 200 mm welded stainless steel sheet.

In order to save on capital and operational cost for small membrane systems, it is anticipated that the ability to perform chemical cleaning *in situ* may not be engineered into small systems' design. For that reason it is essential that modules can be removed and replaced without laborious effort. Flanged-type coupling of modules to manifolds is therefore favoured, as opposed to the bayonet designs originally developed for the 90 mm modules.

6.0 Recommendations

Thus far research and development of capillary membranes concentrated on the development of membranes in the 35 kDa molecular mass cut-off and lower range. Modules that were developed during the course of this programme and earlier programmes concentrated mostly on axial-flow and transverse-flow type modules.

It is recommended that consideration be given to the following areas of research:

Membrane development

Consideration should be given to the development of high molecular mass cut-off membranes as well as microfiltration membranes. These membranes will provide greater flux performance and are suited for use in potable water provision where colour, iron and aluminium removal is not required.

Consideration should also be given to develop ultrafiltration and/or microfiltration membranes from hydrophilised hydrophobic materials. Such membranes will have the chemical and oxidative stability inherent of hydrophobic materials, combined with a lower fouling capacity.

Membrane bioreactors

Membrane bioreactors find increasing application in industrial and domestic wastewater treatment. Consideration should be given to the development of membrane modules that are suitable for use in membrane bioreactor applications. The development of narrow-bore high-flux capillary membranes and flat-sheet membranes and manifolding systems to house the membranes should form part of such a research effort.

Process development

Affinity separation is an attractive approach to remove biologically active compounds from a mixture. Consideration should be given to investigate the usefulness of the approach developed during the course of the project for the detection of endocrine disruptive chemicals in water sources.

Commercialisation

Some of the products developed during the course of the project are ready for commercialisation. Consideration should be given to make the technology available for commercial exploitation.

Ooo OOO ooO

Other related WRC reports available:

Development of specialised cross- and transverse-flow capillary-membrane modules

Domröse SE, Sanderson RD and Jacobs EP

This project was aimed at the further development and industrialisation of specialised cross- and transverse-flow capillary membrane modules for application in the large-scale treatment of surface water to potable standards, and the upgrading of industrial and secondary treated effluents. The results obtained from this project show promise with regard to the commercialisation of membrane technology in South Africa.

The following products resulted from the research:

- A 3 x 50 mm diameter cartridge capillary membrane module (3 x 1.5 = 4.5 m^2 membrane area) was laboratory bench-tested over an extended period of time and successfully field-tested.
- Three 90 mm diameter modules (3 x 5 m^2 = 15 m^2 membrane area), requiring a manifold, were installed and tested for 23 months. Further field trials are being conducted and pilot plants are operating with six modules at two other sites.
- A large 200 mm diameter module cartridge (18 to 25 m^2 membrane area) has been developed as it makes a manifold superfluous. This module has been bench-tested and has exceeded all expectations. Delivery of pure water was measured at over 1 000 L/h.m^2 at a trans-membrane pressure of only 50 kPa. The manufacturing method is being patented and much larger modules are now possible.
- A patent, *Capillary Membrane Modules*, has been filed and granted for an epoxy encapsulation method, SA Patent 96/1580, developed under the project.
- Modules have been developed for containment in larger tanks. 200 mm cartridges can now be housed in a multi-cartridge or tank-type module, creating plants of up to 1 375 m^2 membrane area.

Report Number: 618/1/98 **ISBN: 1 86845 397 9**

Development of transverse-flow capillary-membrane modules of the modular and block types for liquid separation and bioreactors

Domröse SE, Finch DA and Sanderson RD

The transverse-flow membrane modules developed in this project entail an arrangement of capillary membranes in a cross-flow mode with regard to the flow. Transverse-flow membrane modules may be used for many commercial and industrial applications, because of the higher mass-transfer coefficient modular design, individual stacking freedom and possible uses as bioreactors.

A working transverse-flow, capillary membrane module of 24 m^2 membrane area has been developed which has potential for a variety of uses. In addition to the normal separation role, the module may be used to add gases (O_2, CO_2, H_2S) to or strip them from the liquid, thereby providing compelling reasons for its use as a bioreactor. Unfortunately the module is still somewhat sophisticated and might be expensive to manufacture at this stage.

However, the project has paved the way for the production of very large modules, with 200 capillary membranes per layer, 333 layers high (1 m high) which would have surface areas of 250 m^2 for externally-skinned membranes, which can be constructed using the same methods as those used for the present 24 m^2 model. This product is seen to have good potential for a wide range of water-related applications.

Report Number: 847/1/98 **ISBN: 1 86845 412 6**

TO ORDER: Contact **Rina** or **Judas** - Telephone No: 012 330 0340
Fax Number: 012 331 2565
E-mail: publications@wrc.org.za

Water Research Commission
Private Bag X03, Gezina, 0031, South Africa
Tel: +27 12 330 0340, Fax: +27 12 331 2565
Web: http://www.wrc.org.za

1868458431

Designed by The Kashan Group K-2102 (www.kashangroup.com)